iScience

CellPress
OPEN ACCESS

Article

Cerebrospinal fluid exploratory proteomics and ketamine metabolite pharmacokinetics in human volunteers after ketamine infusion

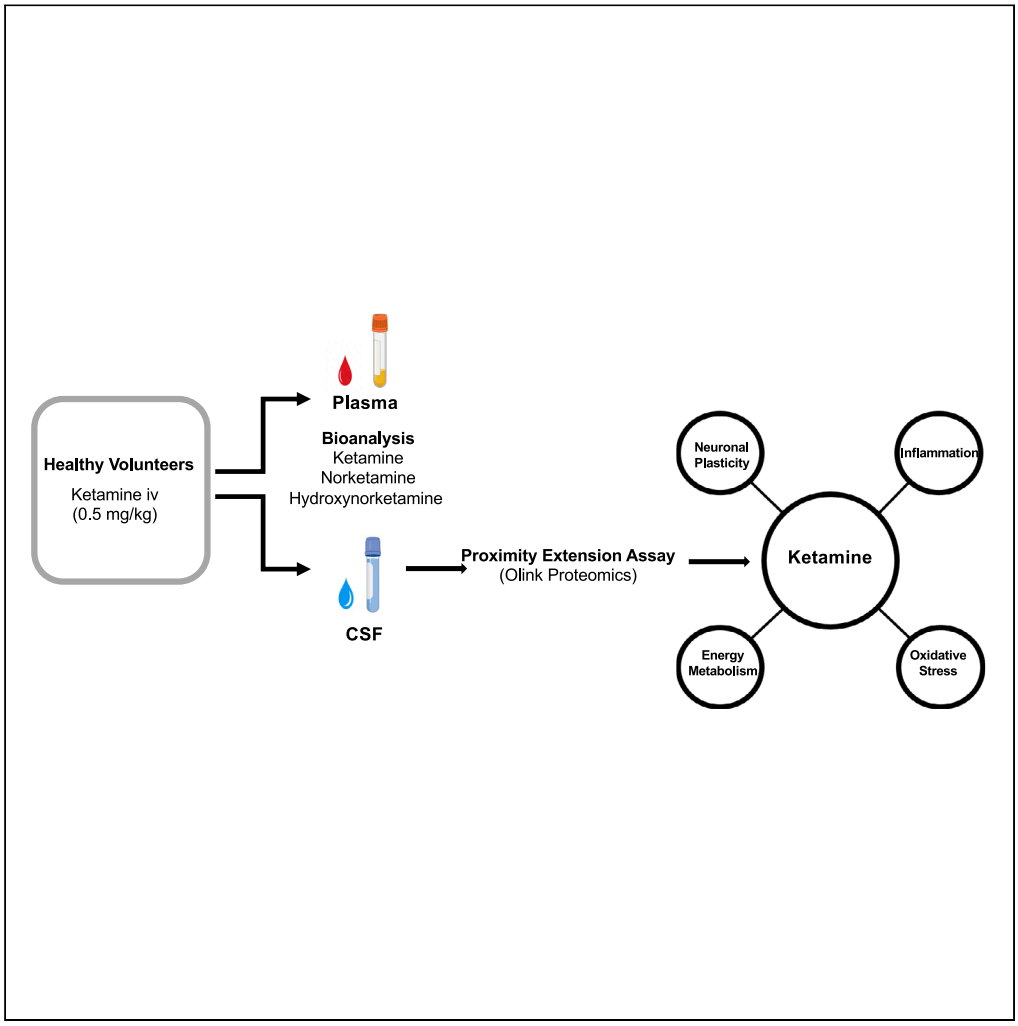

Ruin Moaddel, Cristan A. Farmer, Mani Yavi, ..., Josephine M. Egan, Luigi Ferrucci, Carlos A. Zarate, Jr.

moaddelru@mail.nih.gov

Highlights

Ketamine, norketamine, and hydroxynorketamine cross the blood brain barrier

Ketamine altered expression of ~350 proteins in the CSF at consecutive timepoints

CSF insulin levels increased after ketamine infusion

Ketamine infusion impacted multiple pathways, suggesting pleotropic effects

Moaddel et al., iScience 26, 108527
December 15, 2023 © 2023
https://doi.org/10.1016/j.isci.2023.108527

iScience

CellPress
OPEN ACCESS

Article

Cerebrospinal fluid exploratory proteomics and ketamine metabolite pharmacokinetics in human volunteers after ketamine infusion

Ruin Moaddel,[1,5,*] Cristan A. Farmer,[2] Mani Yavi,[2] Bashkim Kadriu,[2] Min Zhu,[1] Jinshui Fan,[1] Qinghua Chen,[1] Elin Lehrmann,[1] Giovanna Fantoni,[1] Supriyo De,[1] Caio H. Mazucanti,[1] Elia E. Acevedo-Diaz,[2] Peixiong Yuan,[2] Todd D. Gould,[3,4] Lawrence T. Park,[2] Josephine M. Egan,[1] Luigi Ferrucci,[1] and Carlos A. Zarate, Jr.[2]

SUMMARY

Ketamine is a treatment for both refractory depression and chronic pain syndromes. In order to explore ketamine's potential mechanism of action and whether ketamine or its metabolites cross the blood brain barrier, we examined the pharmacokinetics of ketamine and its metabolites—norketamine (NK), dehydronorketamine (DHNK), and hydroxynorketamines (HNKs)—in cerebrospinal fluid (CSF) and plasma, as well as in an exploratory proteomic analysis in the CSF of nine healthy volunteers who received ketamine intravenously (0.5 mg/kg IV). We found that ketamine, NK, and (2*R*,6*R*;2*S*,6*S*)-HNK readily crossed the blood brain barrier. Additionally, 354 proteins were altered in the CSF in at least two consecutive timepoints ($p < 0.01$). Proteins in the classes of tyrosine kinases, cellular adhesion molecules, and growth factors, including insulin, were most affected, suggesting an interplay of altered neurotransmission, neuroplasticity, neurogenesis, synaptogenesis, and neural network functions following ketamine administration.

INTRODUCTION

(*R*,*S*)-Ketamine is a dissociative anesthetic that exerts rapid-acting antidepressant and anti-suicidal effects in individuals with major depressive disorder (MDD),[1] bipolar depression,[2,3] and treatment-resistant depression (TRD).[4–7] Evidence suggests that ketamine's antidepressant effects are mediated by several mechanisms, including α-amino-3-hydroxy-5-methyl-4-isoxazolepropionic acid (AMPA) activation,[8,9] N-methyl-D-aspartate (NMDA) receptor inhibition, disinhibition of pyramidal cells, and an acute cortical glutamate surge. These central, pleotropic effects are then thought to result in the downstream activation of synaptogenesis and neuroplasticity pathways.[10] Moreover, ketamine is effective for the treatment of chronic pain disorders,[11,12] perhaps via mechanisms similar to those responsible for antidepressant effects.

Ketamine and its metabolites are pharmacologically active,[6,13–17] and in preclinical animal model studies, (2*S*,6*S*)-hydroxynorketamine (HNK) and (2*R*,6*R*)-HNK exerted rapid antidepressant-like behavioral effects without functionally inhibiting the NMDA receptor at physiologically relevant concentrations[8,18,19] and without the sensory dissociation, ataxia, or misuse liability associated with ketamine.[3] An initial pharmacokinetic analysis of individuals with treatment-resistant MDD (medication washout) and treatment-resistant bipolar depression (concomitant treatment with either lithium or valproate) receiving a single intravenous infusion of low-dose ketamine found that (2*S*,6*S*;2*R*,6*R*)-HNK was a major circulating metabolite,[20,21] with measurable levels detected 48 h post-ketamine administration. Unexpectedly, a small, randomized, placebo-controlled, crossover trial found that higher (2*S*,6*S*;2*R*,6*R*)-HNK concentrations were related to less of an antidepressant response in humans as assessed via the Montgomery-Asberg Depression Rating Scale (MADRS) at Days 3 and 7 post-treatment.[14] However, the same study found that (2*S*,6*S*;2*R*,6*R*)-HNK was associated with increased gamma power, a biomarker of treatment response.

Most studies investigating ketamine and its metabolites have been conducted in animal models of depression, while similar data in humans have been mainly derived from peripheral blood samples. Notably, because the conversion of ketamine to HNKs does not appear to occur in the brain, brain levels reflect penetrance into brain.[14,22] To date, proteomic studies with ketamine have predominantly been limited to rodent studies.[23] Determining proteomic changes in cerebrospinal fluid (CSF) post-ketamine administration may capture pathway changes that are closer to ketamine's mechanism of action, thereby helping to identify its effects on the central nervous system (CNS). We recently carried out a metabolomic analysis of plasma and CSF samples in healthy volunteers receiving subanesthetic-dose ketamine and identified several pathways that may be relevant to its mechanism of action, including inflammation, the nitric oxide (NO) and mTOR signaling pathways, mitochondrial oxidative capacity, cholesterol metabolism, and sphingolipid rheostat.[24] The present study expands this area of research by

[1]Biomedical Research Center, National Institute on Aging, National Institutes of Health, Baltimore, MD 21224, USA
[2]Experimental Therapeutics and Pathophysiology Branch, National Institute of Mental Health, National Institutes of Health, Bethesda, MD, USA
[3]Departments of Psychiatry, Pharmacology, and Neurobiology, University of Maryland School of Medicine, Baltimore, MD 21201, USA
[4]Veterans Affairs Maryland Health Care System, Baltimore, MD 21201, USA
[5]Lead contact
*Correspondence: moaddelru@mail.nih.gov
https://doi.org/10.1016/j.isci.2023.108527

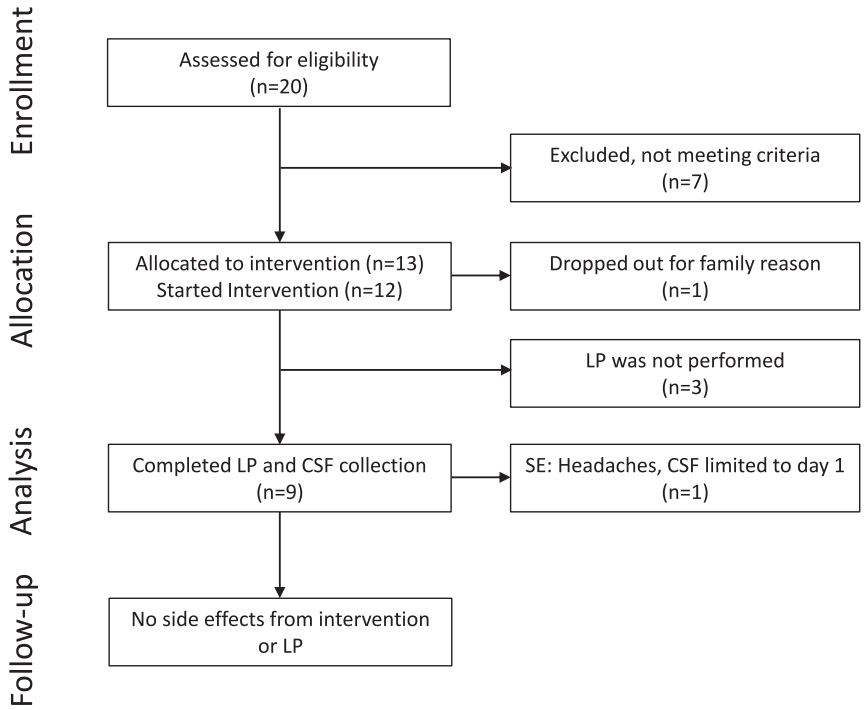

Figure 1. CONSORT diagram.

examining the pharmacokinetics of ketamine and its metabolites in human plasma and CSF (as a brain proxy), as well as CSF proteomic analysis, to provide additional insight into potential mechanisms of action of ketamine and its metabolites.

RESULTS

Concentrations of ketamine, norketamine, and hydroxynorketamines in plasma and cerebrospinal fluid of healthy volunteers (5M, 4F) after IV ketamine infusion (0.5 mg/kg) over 40 min

Ketamine is metabolized to several downstream metabolites including NK, HNK, and dehydronorketamine (DHNK) (Figure S1). The pharmacokinetic profile of ketamine, NK and (2*R*,6*R*;2*S*,6*S*)-HNK was carried out on nine healthy volunteers (CONSORT details are provided in Figure 1, demographic information in Table S1, and a flowchart of the study procedure in Figure 2A) and was similar in plasma and CSF (Figure 2B; Table 1); the CSF:plasma ratio was 0.917, 0.829, and 0.980, respectively, demonstrating that ketamine, NK, and (2*R*,6*R*;2*S*,6*S*)-HNK cross the blood-brain barrier (BBB), with high systemic exposure in both compartments (Table 1). Ketamine, NK, and (2*R*,6*R*;2*S*,6*S*)-HNK had similar profiles, with the peak time (T_{max}) at 40 min for ketamine in plasma and 120 min in CSF, 120 min for NK in plasma and CSF, and between 240 and 360 min for (2*R*,6*R*;2*S*,6*S*)-HNK in plasma and 360 min in CSF (Figure 2B). DHNK levels in the CSF were near the lower limit of quantitation (Figure S2), suggesting that DHNK does not actively cross the BBB. The resolution of (2*R*,6*R*)-HNK and (2*S*,6*S*)-HNK, as well as (R)-NK and (*S*)-NK, demonstrated that they had similar systemic exposure in plasma and CSF (Figure 3), with (2*R*,6*R*)-HNK having a ~0.98 CSF/plasma ratio, (2*S*,6*S*)-HNK having a ~0.94 CSF/plasma ratio, (R)-NK having a ~0.80 ratio, and (*S*)-NK having a ~0.82 ratio (Table S2). This is consistent with previous studies in rodent models that observed a 1:1 ratio of CSF:plasma areas under the curve (AUCs) for (2*R*,6*R*)- and (2*S*,6*S*)-HNK.[6,25,26]

Interestingly, the distribution of the ratio of chiral enantiomers of ketamine metabolites showed increased levels of (2*R*,6*R*)-HNK versus (2*S*,6*S*)-HNK in both CSF and plasma after 240 min and with a higher ratio of (*S*)-NK in plasma until 5 h after administration (Figure 3). This was observed in our study with the increased systemic exposure of (2*R*,6*R*)-HNK over (2*S*,6*S*)-HNK in plasma (~1.22) and CSF (~1.28) and (*S*)-NK over I-NK in plasma (~1.07) and CSF (~1.10). The clear increase of (2*R*,6*R*)-HNK relative to (2*S*,6*S*)-HNK over time in CSF and plasma may indicate increased clearance of (2*S*,6*S*)-HNK, which would be consistent with the previously reported increased clearance of (*S*)-ketamine.[27] The enantiomer-specific divergent distribution may suggest that (2*R*,6*R*)-HNK plays a more prominent role in ketamine's sustained antidepressant effects because measurable levels of HNK were observed one day after infusion (Figure 2B). No robust association was observed for ketamine and its metabolites in CSF or plasma and its dissociative side effect profile (as assessed via the Clinician-Administered Dissociative States Scale (CADSS)). Some evidence was observed for an association between a higher CSF:plasma ratio of ketamine and higher amnesia, derealization, and total CADSS scores (Figure S3), suggesting that BBB penetration is important, rather than circulating plasma or CSF levels *per se*.

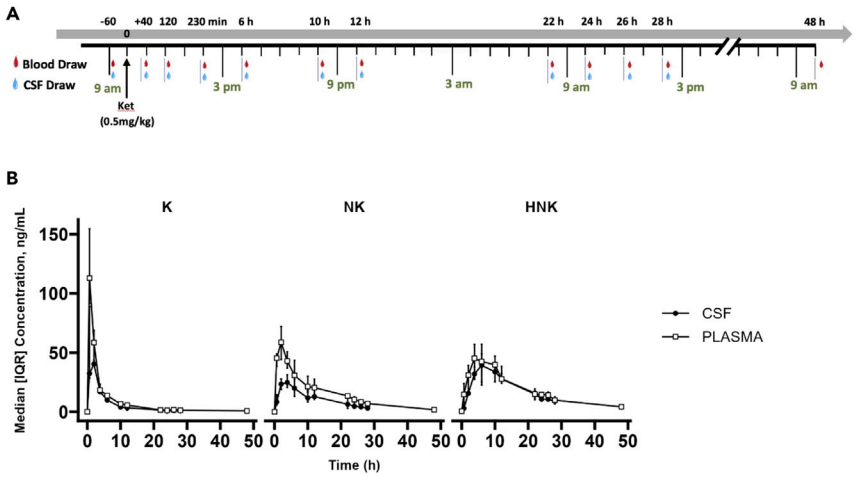

Figure 2. Flow chart and circulating levels of ketamine and downstream metabolites in plasma and CSF of healthy volunteers after IV ketamine infusion (0.5 mg/kg) over 40 min

(A) Study procedures for ketamine infusion and subsequent time points of blood and CSF draws.

(B) Ketamine (K), norketamine (NK), (2*S*,6*S*;2*R*,6*R*)-hydroxynorketamine (HNK) levels in CSF and plasma post-ketamine infusion, where median and interquartile range (IQR) are provided .

Proteomic analysis of cerebrospinal fluid following ketamine infusion

An exploratory proteomic analysis was carried out on the CSF collected at multiple timepoints (baseline, 40, 120, 230, 360, 720, and 1,440 min) following ketamine infusion. In this study of the 1460 proteins, the relative concentrations of 1108 were detected in CSF with >30% above the limit of detection (LOD). Of those, 354 proteins had at least two *sequential* timepoints with significantly different levels compared to baseline at p value of <0.01, with 345 increasing and nine decreasing over baseline following ketamine infusion (Table S3). No vehicle control was carried out to compare CSF proteomic changes between vehicle and the ketamine group. However, it is assumed that changes resulting from an acute response to the infusion and/or placement of the intrathecal catheter would occur at earlier timepoints. It is thus possible that changes occurring at later time points could result from a homeostatic response in healthy individuals to the acute response.

Proteins with T_{max} at or before 2 h post-ketamine infusion

After ketamine infusion, adverse events are typically observed within 2 h post-administration, and initial antidepressant effects are also reported to occur by the 2-h timepoint post-infusion (Figure 4). In our study, six proteins (SCLY, LILRB5, VTA1, CXCL8, IL1RN, and RNF41) increased at 40 min after drug administration, with only five proteins (ITGB2, SCLY, BLVRB, CASP3, and HARS1) peaking at 2 h, consistent with the timing of ketamine's antidepressant effects. ITGB2 suppresses inflammation and immune activation[28]; SCLY is associated with the reduction of depressive symptoms[29] and also plays a role in modulating cellular redox along with BLVRB[30]; and the increase of CASP3 and HARS1 is consistent with a previous animal study where ketamine increased cyclin D1 and cleaved CASP3 levels.[31]

Proteins with T_{max} where antidepressant effects were observed (from four to 24 h post-ketamine infusion)

In the CSF, the following patterns were observed. Alterations in 56 proteins (15.8% of identified proteins; 54 increasing, two decreasing relative to baseline levels) began to appear at the 2-h timepoint post-ketamine; alterations in 154 proteins were observed at 4 h (43.5%; 150 increasing, four decreasing); alterations in 65 proteins were observed at 6 h (18.4%; 64 increasing, one decreasing); and alterations in 73 proteins were observed at 12 h (20.6%; 71 increasing, two decreasing) (Table S3). CSF levels of the ketamine metabolite (2*R*,6*R*;2*S*,6*S*)-HNK peaked 6 h post-administration (Figure 2). As already noted above, the antidepressant effects of ketamine have been reported to begin by 2 h after infusion, continue for several days, and are maximal at 24 h.[7] In this study, we therefore aligned protein changes related to inflammation, oxidative stress, energy metabolism, and neuronal plasticity with ketamine's known timing of antidepressant effects (Figure 4). These effects are consistent with the observations seen in the healthy volunteers, where 19 proteins peaked at 4 h, seven proteins peaked at 6 h, 111 proteins (31.4%) peaked at 12 h, and 212 proteins (59.9%) peaked at 24 h. String analysis was carried out on the proteins that peaked at 12 h (Figure 5) and 24 h (Figure 6) separately to identify central hubs for each maximal timepoint with the full string network, active interaction sources (Textmining, experiments, databases, co-expression, neighborhood), highest confidence (0.900).

4E-BPs (EIF4EBP1), putative key effectors for the antidepressant activity of both ketamine and (2*R*,6*R*)-HNK via mechanistic target of rapamycin complex 1 (mTORC1),[32] were increased in the CSF and had reached peak levels by 4 h. Similarly, HMOX1 protein levels peaked at 4 h. Decreased expression of HMOX1 has been associated with depressive symptoms.[33] GUSB, a lysosomal acid hydrolase responsible for the catalytic deconjugation of β-*d*-glucuronides and a potential biomarker for early response of antidepressants to glioma treatment, was also increased post-infusion. The increased PEAR1 levels observed in the CSF are also consistent with its observed increase in

Table 1. Pharmacokinetic (PK) parameters of ketamine and downstream metabolites in the plasma and CSF of healthy volunteers after IV ketamine infusion (0.5 mg/kg) over 40 min

		CSF			Plasma		
Metabolite	PK Parameter	n	Median [IQR]	Range	n	Median [IQR]	Range
K	C_{max} (ng/mL)	9	42.36 [39.25, 89]	32.39–94.47	8	112.87 [91.52, 155]	85.34–247.51
K	T_{max} (min)	9	120 [40, 120]	40–120	8	40 [40, 40]	40–40
K	AUC (ng.min/mL)	9	2742.64 [2131.41, 2773]	1695.98–3022.87	8	2990.36 [2523.72, 3286]	2104.85–4006.24
K	half.life (min)	8	545.5 [403.45, 689]	355.95–849.07	8	592.99 [449.01, 765]	208.78–898.04
NK	C_{max} (ng/mL)	9	25.26 [20.93, 32]	16.3–42.15	8	59.27 [48.39, 72]	35.21–78.34
NK	T_{max} (min)	9	120 [120, 120]	120–230	8	120 [100, 148]	40–230
NK	AUC (ng.min/mL)	9	3997.96 [3379.25, 4342]	1840.97–4393.29	8	4820.98 [3949.2, 5331]	2389.11–5592.8
NK	half.life	9	778.73 [558.11, 1548]	121.71–1928.62	8	1200.23 [976.09, 1586]	606.23–4202.75
HNK	C_{max} (ng/mL)	9	39.26 [30.03, 49]	9.02–65.36	8	46.19 [28.06, 58]	12.02–70.56
HNK	T_{max} (min)	9	360 [230, 360]	230–600	8	295 [230, 420]	230–600
HNK	AUC (ng.min/mL)	9	5023.72 [4211.75, 5121]	2588.38–5451.1	8	5126.06 [4250.94, 5339]	2812.12–5947.81
HNK	half.life (min)	9	2267.35 [1851.63, 2819]	1290.69–3593.57	7	2215.58 [2172.04, 2415]	1190.54–3248.11

C_{max}, maximum concentration; T_{max}, timepoint of maxium concentration (minutes).

polymorphonuclear leukocytes in individuals with treatment-resistant depression following electroconvulsive therapy (ECT).[34] An increase in leukocyte inhibitory factor (LIF; an interleukin 6 class cytokine known to affect cell growth) observed in our study has been shown to prevent colitis-induced depressive-like behavior.[35] NRCAM, a transmembrane protein located on the cell surface involved with cell-cell and extracellular matrix (ECM) attachment,[36] decreased following infusion (T_{max} = 24 h). This finding is particularly relevant to ketamine infusions because previous studies reported decreased NRCAM levels in patients with MDD.[37] Conversely, NPTXR, which has been reported to be lower in the CSF of patients with MDD,[38] was decreased following infusion. Interestingly, EPCAM, a surface marker for pluripotent human embryonic stem cells, was increased following infusion; EPCAM is present on exosomes, and its overexpression induces cell proliferation.[39]

Several of the changes that occurred at or after 4 h post-infusion are consistent with previous studies demonstrating ketamine's role in modulating inflammation, cellular redox, energy homeostasis, and neuronal plasticity.

Inflammation

Proteins related to inflammation, including chemokines, cytokines, interleukin receptors, HMOX1, VTA1, LILRB2, and CXCL1[40,41] were identified following ketamine infusion at several timepoints, including at 4 h post-infusion. NEFL also peaked at 4 h, however, with a $0.01 < p < 0.05$. IL1RN and CXCL8 peaked at 6 h post-infusion; IL19, IL1RL1, IL1RL2, IL6, CCL2, CCL17, CXCL16, CSF1, and MMP1 peaked at 12 h post-infusion; and IL10RB, IL15, IL17RA, IL18BP, IL18R1, IL6R, and IL6ST peaked at 24 h post-infusion. HMOX1 has been reported to have anti-inflammatory properties and is inducible by nitric oxide (NO),[42] consistent with our previous studies suggesting increased NO production following ketamine.[43] The increase of CXCL8 and IL1RN likely result from an acute response, as CXCL8 and IL1RN began increasing by 40 min. Changes were observed for both LILRB2 and LILRB5, both of which are expressed in immune cells, with LILRB2 expressed in monocytes, macrophages, and dendritic cells[40] and LILRB5 expressed in macrophages.[41] Interestingly, in an animal model, memory deficits by oligomeric Aβ were mediated by loss of synaptic plasticity in a LILRB2-dependent manner.[40] The observed increase of CCL2 may not be beneficial in healthy volunteers and is inconsistent with the reported anti-inflammatory effects of ketamine[44]; in depressed individuals, however, it may play a role in the balance of excitatory and inhibitory cortical activity.[45] Increased IL6 was consistent with the increase reported in whole hippocampus of mice following ketamine infusion.[46] The increase of CSF1 could also suggest adverse effects, as CSF1 can induce microglial activation contributing to depression[47]; however, it has also been reported to exert anti-inflammatory effects in a variety of nervous system diseases via CSF1R and the CSF1R/PLCG2/PKCε/CREB signaling pathways.[48] IL6 and CSF1 have also been shown to influence the proliferation of neural stem/progenitor cells.[49]

The anti-inflammatory protein tissue inhibitor of metalloproteinase 3 (TIMP3 (T_{max} = 12 h)) began to increase 4 h after ketamine infusion, and ADAMTS8 was also increased by 4 h post-infusion. TIMP3 is known to inhibit multiple metalloproteinases (MMPs, ADAMs, and ADAMTSs), but we cannot ascertain whether the increase of TIMP3 was a direct result of ketamine infusion or a homeostatic response to the increase of ADAMTS8 in our healthy volunteers. While several of these observed changes are consistent with ketamine's anti-inflammatory effects,[44] the increase of several pro-inflammatory cytokines and chemokines is of interest. Cytokines play crucial roles in the communication between neurons and glia, and in brain-periphery interactions,[50] and they directly modulate long-term potentiation (LTP) in neurons.[50] Membrane depolarization and NMDA receptor (NMDAR) activation are needed to establish LTP.[50] Increased brain cytokine levels occur under several conditions of traumatic brain injury and neurodegeneration and, when unchecked, can impair neuronal function in the adult brain[50]; in addition, evidence suggests that inflammatory-type cytokines play physiological roles in the brain in the absence of stress-type challenges.[50] For example, TNFα is involved in a homeostatic form of plasticity that regulates neuronal firing rate by altering the quantity of

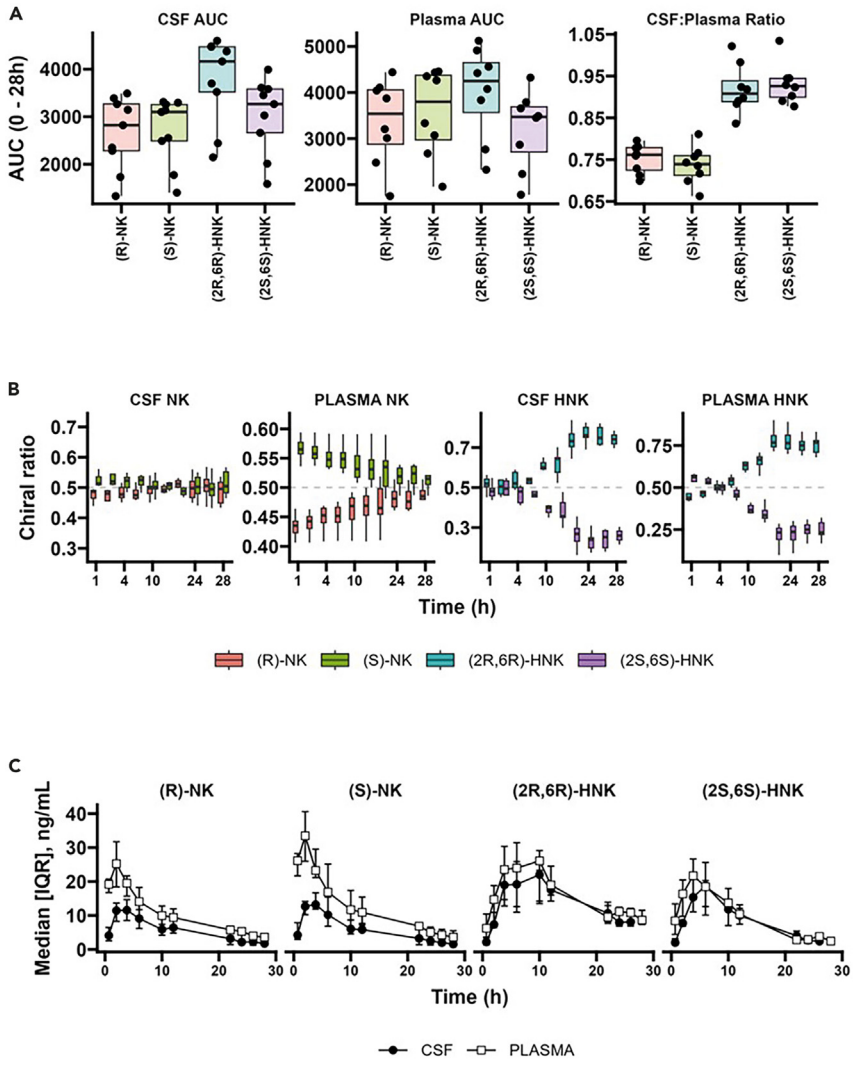

Figure 3. Circulating levels of the enantiomers of ketamine metabolites, norketamine (NK), and hydroxynorketamine (HNK) in the plasma and CSF of healthy volunteers after IV ketamine infusion (0.5 mg/kg) over 40 min

(A–C) (A) Area under the curve (AUC), (B) the percentage of the enantiomers over total, and (C) the resolution of (2*R*,6*R*)-HNK, (2*S*,6*S*)-HNK, (*R*)-NK, and (*S*)-NK in plasma and CSF at various timepoints through 1,680 min (28 h) post-ketamine infusion, where median and interquartile range (IQR) are provided.

postsynaptic AMPA receptors,[50] and several inflammatory cytokines have been shown to contribute to synaptic plasticity and facilitate LTP and memory consolidation.[50] Both VTA1 and CA1 increased following ketamine infusion, and both are involved in homeostasis regulation[51,52]; in particular, VTA is an important regulator of endosomal-lysosomal function,[53] and CA1 plays a role in cellular respiration and in brain processes for the transmission of neuronal signals.[52]

Other proteins related to inflammation included KYNU and NMNAT; however, these had a $0.01 < p < 0.05$. The changes observed for KYNU and NMAT are consistent with our previous study that found an association between the kynurenine metabolome, indoleamine 2,3-dioxygenase (IDO) activity, nicotinamide adenine dinucleotide (NAD^+) biosynthesis, and ketamine administration.[24] While NAMPT activity (NMN/NAM ratio) was found to decrease in (2*R*,6*R*)-HNK treated mice,[24] its levels seemed unaffected in the CSF in our study. Interestingly, KYNU and SIRTs have been associated with depressive symptoms,[54] and in this study SIRT2 also increased following ketamine infusion (T_{max} = 24 h). The increase of SIRT2 suggests the inactivation of the NLRP3 inflammasome.[55]

Oxidative stress

Several proteins related to cellular redox (HMOX1, CSTB)[56] (T_{max} = 4 h) and RBP2 (T_{max} = 6 h) increased following ketamine infusion. HMOX1 reduces oxidative stress via the heme oxygenase reaction pathway,[33] and RBP2 could result in an increase of antioxidants (retinol and retinyl esters).[57,58] CSTB is present in the synaptic region and is also involved in synaptic plasticity.[56] It is secreted under depolarizing conditions[56] and

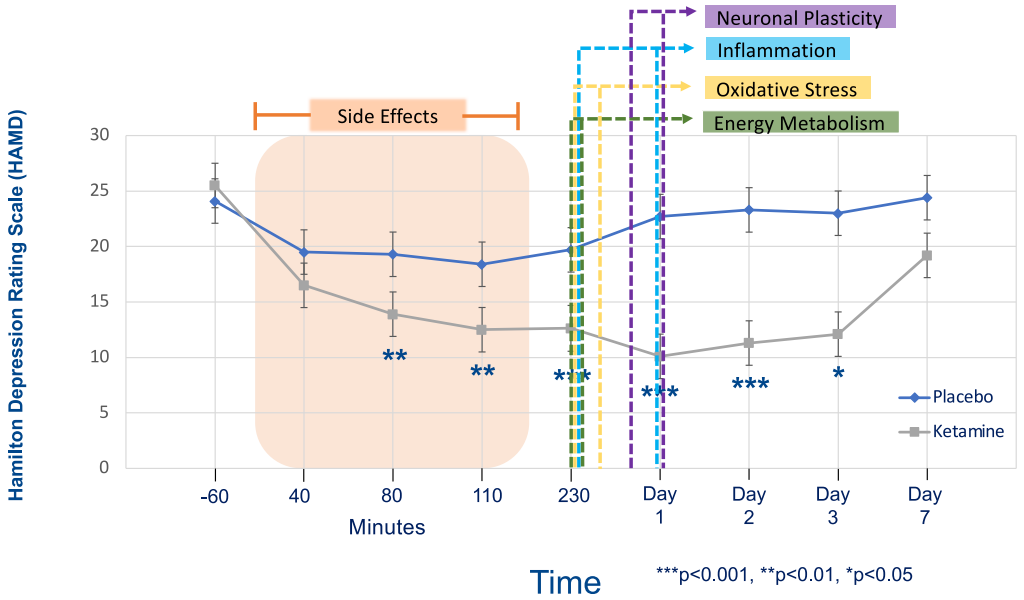

Figure 4. The rapid antidepressant effects of ketamine in unmedicated individuals with treatment-resistant depression overlayed with CSF proteomic changes observed in healthy volunteers (n = 9) after IV ketamine infusion (0.5 mg/kg) over 40 min
(Adapted from[7]).

interacts strongly with SOD-1, an antioxidant protein,[56] which also increased following ketamine infusion (T_{max} = 24 h). Surprisingly, ketamine infusion increased cathepsin CTSB, which is thought to link oxidative stress to the activation of the NLRP3 inflammasome.[59] Disruption of the cathepsin functions is thought to contribute to MDD, bipolar disorder, and schizophrenia.[60] CTSB, however, has also been shown to improve cognition and memory function in humans.[60] Cathepsins play roles in cellular homeostasis, lysosomal degradation, and autophagy.[60]

In addition to CTSB, CTSL (T_{max} = 12 h) and CTSS (T_{max} = 24 h) also increased following ketamine infusion, $0.01 < p < 0.05$. CTSB and CTSL have been shown to induce axonal growth in neurons and to mediate astrogliosis and neuroprotection.[60] The increase in cathepsins also suggests an increase in lysosomal membrane permeabilization.[61,62] Accordingly, LIMP2 (SCARB2) increased following ketamine administration. LIMP2 is required for maintenance of lysosomes and endosomes,[63] and its overexpression has been shown to improve lysosomal glucosyl ceramidase activity.[64] Conversely, LIMP-2 deficient mice were characterized by a peripheral demyelinating neuropathy, associated with a loss of myelin proteins and an increased activity and expression of lysosomal proteins.[65] Other lysosomal proteins that increased following ketamine infusion included LAMP2 (T_{max} = 12 h), which is necessary for chaperone-mediated autophagy.[66] These results are in accordance with our recent metabolomic study in the same participants,[24] where increased sphingomyelin (SM) levels were observed in the CSF, suggesting increased lysosomal membrane permeabilization. Bone morphogenetic proteins (BMPs), cofactors that enhance acid sphingomyelinase (ASM) activity,[61] also increased following ketamine infusion (BMP6). ASM can impact myelination and cell differentiation/proliferation in the CNS and has been associated with MDD.[67] BMPs are expressed in the choroid plexus, and BMP6 is expressed in the hippocampus and substantia nigra and in most cell types (neurons, astrocytes, and oligodendrocytes).[68] The increase of BMP6 is consistent with increased neuronal plasticity reported to occur following ketamine administration, as BMPs play key roles in adult neurogenesis and gliogenesis and regulate energy balance and metabolism in the CNS.[68] Other proteins of interest include the increase of CNDP1 and FKBP4; CNDP1 has been reported to be decreased in the CSF of individuals with MDD, bipolar disorder, or schizophrenia,[38] and FKBP4 is a biomarker of psychiatric disorders.[69]

Energy metabolism

Several changes were consistent with ketamine involvement in energy metabolism,[70] including increases in PPCDC, RBKS, and ENTPD2. An increase in PPCDC, one of the four enzymes involved in the synthesis of CoA, increases CoA levels and modulates cellular energy metabolism.[71] RBKS catalyzes the phosphorylation of ribose to ribose-5-phosphate[72] and is necessary for synthesis of ATP and GTP via the pentose phosphate pathway.[73] The increase of the ecto-nucleosidase ENTPD2, which hydrolyzes 5′-triphosphates, is consistent with ketamine's role in energy metabolism. ENTPD2 degrades extracellular ATP to ADP, thereby preventing prolonged agonist exposure and receptor desensitization and allowing for the replenishment of ADP for re-phosphorylation.[74] Ecto-5′-nucleotidase have been shown to play a role in tissue homeostasis and in acute and chronic inflammation.[75] Alterations in purine metabolism are thought to be involved in depression, as chronic use of fluoxetine and nortriptyline was found to alter ecto-nucleotidase activity in the hippocampus and cortex.[74] All these changes support increased mitochondrial activity, consistent with previous reported mechanisms of action of ketamine.[24] Also consistent with these findings, SHMT1, which converts serine and tetrahydrofolate (THF) to glycine and 5,10-methylene THF, respectively, and is involved in one-carbon metabolism,[76] increased following ketamine infusion.

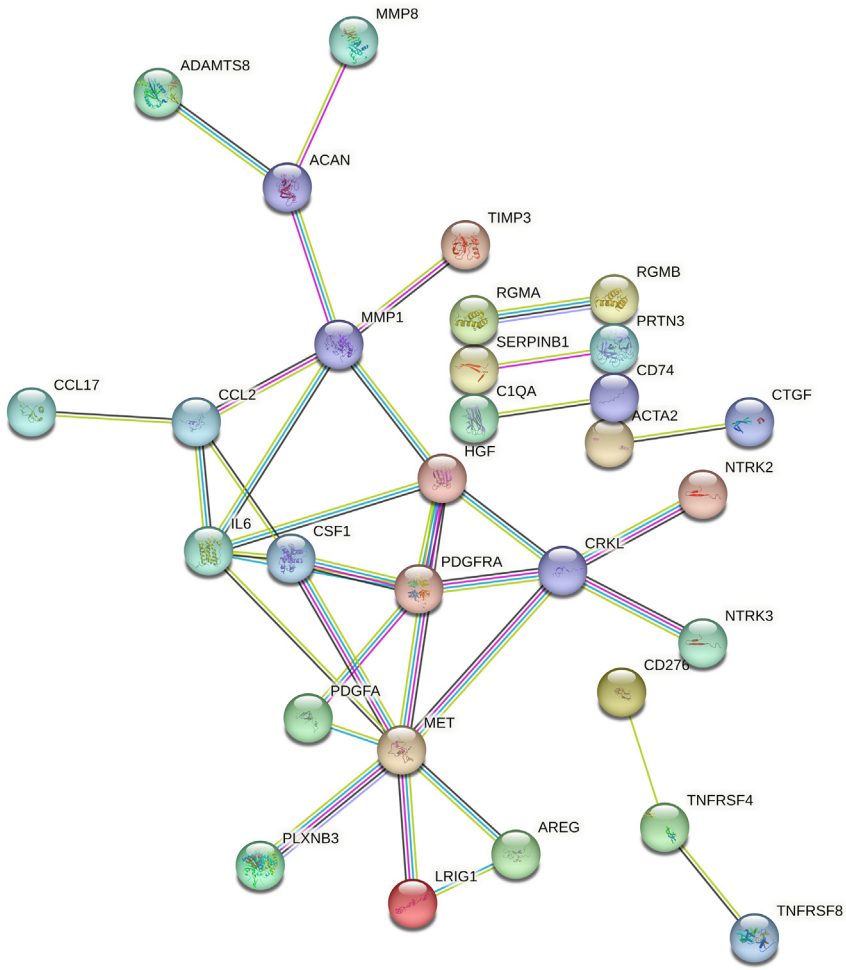

Figure 5. Network representation of differentially expressed proteins in the CSF of healthy volunteers (n = 9) with a maximal increase 12 h after IV ketamine infusion (0.5 mg/kg) over 40 min

STRING analysis for proteins with maximal increases 12 h post-infusion (108 proteins) using the full STRING network, active interaction sources (Textmining, experiments, databases, co-expression, neighborhood), highest confidence (0.900).

Alterations in proteasome expression have been suggested to play a role in MDD, Alzheimer's Disease (AD), schizophrenia, and bipolar depression.[77] In this study, both GLO1 and PSME2, a multi-catalytic proteinase complex, increased following infusion. The increased expression of GLO1 suggests a role for ketamine in the detoxification of the cytotoxic byproduct of glycolysis, which may reduce protein modifications (such as AGEs), oxidative stress, and apoptosis via methylglyoxal.[78]

Neuronal plasticity

Twenty-five receptor tyrosine kinases (RTKs) (16 with T_{max} = 24 h) and five non-receptor tyrosine kinases (NRTKs) were increased at 12 and 24 h post-infusion, several of which were central hubs (12 h post-infusion: CRKL, PDGFRA, MET, HGF; 24 h post-infusion: RTKs: ITGB1, VEGFA, IGF1R, NRP1, NRP2, PDGFRB, FGF5, FGFR2, and RNF41/NRTKs: EGFR, ERBB3, ERBB4, PXN; CAMs: L1CAM, NCAM1, NCAM2, and ALCAM). RTKs and NRTKs control the expression, subcellular distribution, protein-protein interactions, and function of both non-modified and modified proteins and are critically involved in cell survival and function.[79] NRTKs, cytosolic enzymes that are linked to and regulate multiple signal transduction cascades, are enriched at synaptic sites and involved in synaptic plasticity.[79] The increase of the MET NRTK following ketamine administration has been reported to result in improved neuronal growth, dendritic branching, arbor complexity, and spine density.[80] An increase in MET is of further interest because low MET expression is believed to be associated with the altered cognition, social and language skills, and deficient executive functions observed in autism spectrum disorder (ASD),[80] suggesting that ketamine treatment might have therapeutic benefits in ASD. This is further supported by the observed increases in several growth factors and RTKs, including IGF-1R. RTKs, in general, are cell surface receptors for growth factors, cytokines, and hormones that transmit ligand-mediated extracellular signals to cytoplasm and nuclei,[79] and are essential for normal adult tissue function and homeostasis.[81] Several of the RTKs identified in our

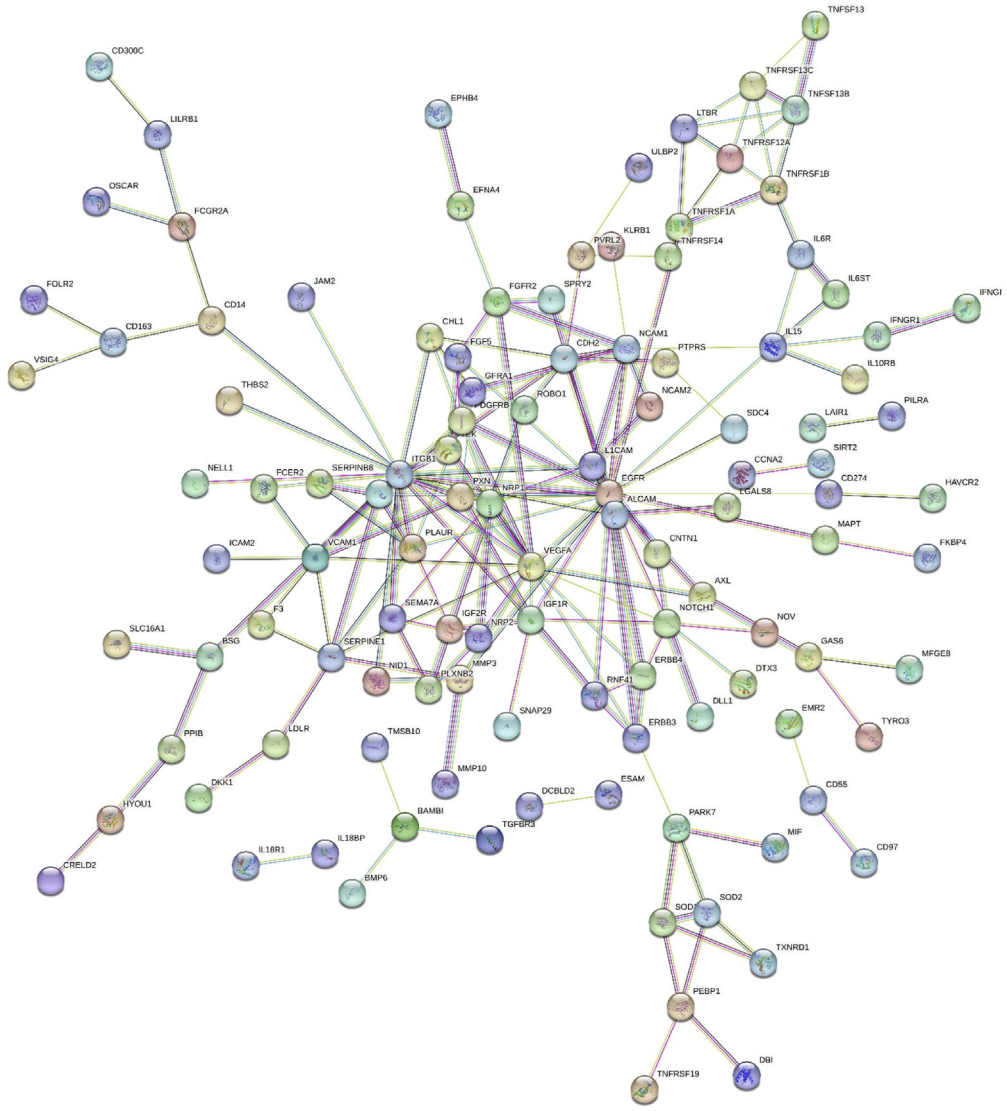

Figure 6. Network representation of differentially expressed proteins in the CSF of healthy volunteers (n = 9) with a maximal increase 24 h after IV ketamine infusion (0.5 mg/kg) over 40 min

STRING analysis for proteins with maximal increases 24 h post-infusion (206 proteins) using the full STRING network, active interaction sources (Textmining, experiments, databases, co-expression, neighborhood), highest confidence (0.900).

analyses play roles in promoting motor neuron survival and axon growth[81] and may have roles to play in MDD. For example, ITGB1was recently identified as a central hub gene in both MDD and AD.[82] An increase in ITGB1 is consistent with an increase in synaptic formation and maintenance and synaptic plasticity,[82] consistent with the robust increase in gamma power observed in healthy volunteers following ketamine treatment.[83] EGFR is also involved in growth, differentiation, maintenance and repair of various tissues and organs.[84] A parallel increase of EGF expression ($p < 0.05$) was also observed in our study. In addition to the RTKs and NRTKs, 28 growth factors also increased following ketamine infusion (Table S4), including 26 that peaked between 12 and 24 h. The concomitant increases of EGF/EGFR, RTKs, growth factors, and NRTKs suggests a "rewiring" of the brain networks following ketamine infusion.[85]

In view of recent research pointing to insulin synthesis and secretion in the epithelial cells of choroid plexi[86] coupled to the increases in RTK protein levels observed in our study – the insulin receptor is a classic RTK – we measured insulin levels in the CSF. We found that CSF insulin levels increased ~3– to 4-fold in all nine participants ($p = 0.0117$) at 12 h, and that levels were still elevated at 24 h (~2-fold increase) ($p = 0.10$; one participant's insulin concentration had returned to slightly below baseline, while others were still above baseline) (Figure 7, Figure S4).

The activation of EGFR and NOTCH1 pathways, observed following ketamine infusion, further suggests maintenance of neural stem cells and neural progenitor cells,[84] with the NOTCH signaling pathway improving depressive symptoms in an animal model by promoting neuronal regeneration in the hippocampus.[87] Ketamine is known to modulate ZIC5 expression by activating the NOTCH signaling pathway.[88] NOTCH

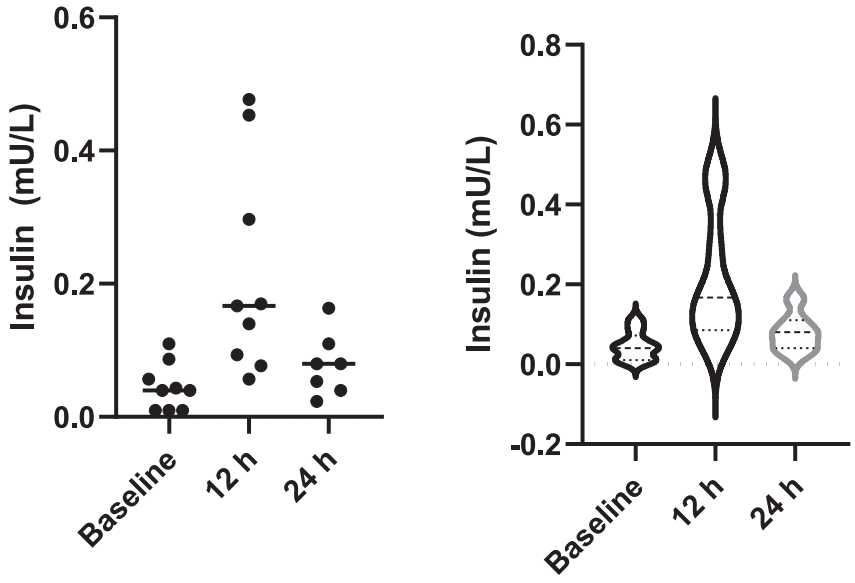

Figure 7. Circulating levels of insulin in the CSF of healthy volunteers after IV ketamine infusion (0.5 mg/kg) over 40 min

(A) CSF insulin levels (mU/L) at baseline, 12 h, and 24 h post-ketamine infusion.

(B) Violin plot illustrating insulin levels between different timepoints.

responsiveness is related to the composition of the ECMs, several of which increased in our study following ketamine infusion, such as SERPINE1, CTSB, CCL2, and TIMP3.[89] Modulation of ECM has been proposed as a mechanism of ketamine's antidepressant effects via increased synaptogenesis.[36] In fact, it has been suggested that ketamine modulates ECM components in part through the orchestration of WNT and TGFβ signaling pathways and the regulatory network of the transcription factor BLMP-1.[36] Cell adhesion molecules (CAMs) are involved in cell-cell and cell-extracellular matrix binding. In our study, 10 CAMs were modulated by ketamine infusion; nine CAMs were increased (NCAM1, NCAM2, VCAM1, ALCAM, ICAM2, ICAM5, BCAM, EPCAM, and L1CAM), with seven having a T_{max} = 24 h, and only NRCAM was decreased post-infusion. CAMs play a role in the processes of neurite pruning and wiring specificity during circuit reassembly.[90,91] The concomitant increase of other CAMs, including integrins and junctional adhesion molecules (JAMs), further supports ketamine's role in neuronal remodeling that is essential for shaping the connectivity of functional circuits.[85,91] This was further demonstrated by the increase of MMPs (MMP3, MMP10, MMP1 (T_{max} = 12 h), MMP8 (T_{max} = 12 h), and MMP-12 (T_{max} = 12 h ($p < 0.05$)), as they mediate structural changes of dendritic spines and axon/dendrite structures.[92] The increase of BSG also supports an increase in neural network formation, as it has been shown to be required for complex dendrite formation in *Drosophila*.[93] The increase in FYB1, which associates with FYN, modulates excitatory synaptic transmission and plasticity and plays a critical role in myelination and in the regulation of glutamate receptors.[94,95]

Integrins link the ECM to the intracellular environment and are implicated in the Reelin signaling pathway,[96] which is required for dendrite development through the activation of mTOR and S6 kinase 1 (S6K1) during cortical development.[97] The Reelin pathway also has a role in the adult brain. For example, the administration of exogenous Reelin, a glycoprotein, improved synaptic plasticity and cognitive behavioral deficits in an adult mouse model of Angelman syndrome.[98] Of relevance to the present study, the disruption of Reelin-mediated synaptic signaling interfered with ketamine's antidepressant actions.[97] The increase of CRKL may indicate the modulation of the Reelin-Dab1-Crk/CrkL pathway following ketamine infusion.[99] Reelin is also secreted by a subpopulation of gamma aminobutyric acid (GABA)-ergic neurons[100] and therefore may play a role in the maintenance of baseline NMDA receptor function.[97] Further supporting the increased formation of synaptic contacts and repair of damaged synapses by ketamine, an increase in PLAU and PLAUR was observed following infusion.[101] The binding of PLAU to PLAUR has been reported to activate the Wnt-β-Catenin pathway in cerebral cortical neurons.[101] PLAU is located in the synapses of excitatory neurons in adult brains, and a decrease in the abundance of PLAU has been observed in the synapse of patients with AD.[101]

Neurotrophic receptor NTRK2 and NTRK3 also interacted with CRKL (Figure 4). NTRK2 binds BDNF and neutrophin-4 while NTRK3 binds neutrophin-3.[102] NTRK2 is mainly located in the adult cortex, cerebellum, striatum, and hippocampus while NTRK3 is mainly expressed during neuronal development.[102] The activation of these TK receptors promotes and regulates the growth and elongation of dendrites and axons.[102] An increase in the PDGF/PDGFR signaling pathway was also observed (both PDGFA and PDGFRA increased), consistent with its association with neuropsychiatric[103] and neurodegenerative disorders.[104]

DISCUSSION

To the best of our knowledge, this analysis is the first human study to assess the pharmacokinetics of ketamine's primary metabolites and their enantiomers centrally in the CSF and to correlate them with psychotomimetic symptoms and protein expression levels over a period of 28 h. Our findings strongly suggest that ketamine, NK, and HNK readily cross the BBB, as they had similar distribution in plasma and CSF.

In addition, (2*R*,6*R*)-HNK had higher systemic exposure in both plasma and CSF than (2*S*,6*S*)-HNK, suggesting that (2*R*,6*R*)-HNK may have higher brain exposure. This would be consistent with previous work showing that ketamine metabolism to (2*R*,6*R*;2*S*,6*S*)-HNK was essential for ketamine's antidepressant effects in mice and that (2*R*,6*R*)-HNK appeared to be primarily responsible for those antidepressant actions.[8] An exploratory study in TRD participants who received a ketamine infusion found an association between an increase in the maximum observed concentration (C_{max}) of (2*S*,6*S*;2*R*,6*R*)-HNK and an increase in whole-brain magnetoencephalography gamma power.[14] In our recent study, a targeted metabolomic analysis was carried out on the CSF and plasma of the same healthy volunteers studied here, and multiple pathways were associated with ketamine's mechanism of action in both the metabolomic[24] and current exploratory proteomic study, including inflammation, oxidative stress, NO signaling pathway, sphingolipid rheostat, and NAD+. Additional changes observed in this study included the activation of the microglial network, increased myelination, cellular proliferation, homeostasis regulation, modulation of proteasome expression, and cellular energy metabolism.

Interestingly, changes in CSF proteins predominantly peaked at 12 h (111 proteins) and 24 h (212 proteins) post-infusion in healthy volunteers, in line with the maximal antidepressant effects reported with ketamine (Figure 4). A large number of these were RTKs, NRTKs, CAMs, and growth factors (including insulin), supporting an increase in synaptic plasticity, neurogenesis, and neural circuit remodeling following ketamine administration.[90,91,97,105] An increase in synaptic plasticity is consistent with our previous study that found increased gamma power six to 9 h post-ketamine infusion in healthy volunteers and MDD participants.[83] Reduced power of oscillations in the gamma frequency band has been observed in depression[106] and in neurodegenerative diseases.[107,108] Multiple synaptic mechanisms play a role in regulating gamma oscillations, including AMPA receptor-mediated depolarization and GABA-A receptor-mediated inhibition,[83] with an effect on balancing excitatory and inhibitory input (E/I balance). In line with these mechanisms, the Reelin signaling pathway was also implicated in ketamine's mechanism.

The increase in CSF insulin after ketamine infusion in our study is of interest, as the prevalence of depression and anxiety in people with type 2 diabetes (T2DM) is reported to be twice the non-diabetic population average and correlates with the severity of insulin resistance.[109] This is also consistent with another recent study, where a combination treatment of lithium and ketamine resulted in upregulated insulin signaling in the infralimbic subregion of the prefrontal cortex.[110] Further, the loss of or a deficient insulin receptor signaling in astrocytes in transgenic mice was shown to reduce evoked dopamine release in the nucleus accumbens and resulted in anxiety- and depressive-like behaviors.[111] Insulin is synthesized and secreted in the epithelial cells of the choroid plexus (CPEs), the same cells that synthesize transthyretin; its secretion is not stimulated by glucose, but by 5-HT through its activation of 5-HT2C receptors on CPEs that results in increased intracellular calcium.[86] Based on these preliminary findings, one of the acute beneficial effects of ketamine infusion on depression and anxiety may result directly from increased insulin secretion from CPEs, as a result of increased central 5-HT secretion (ketamine is known to increase 5-HT release from the medial prefrontal cortex of mice[112]) or by an unknown mechanism. Subsequent insulin receptor activation in astrocytes and neurons results in increased dopamine release in the nucleus accumbens[111] as well as NO generation, leading to downstream effects on synaptic plasticity and neuronal rewiring.

Following on from the insulin observations, RTK-activating growth factors (28 proteins), as a whole, exert anabolic effects and promote cell survival, growth, and metabolism.[113] The PI3K/AKT/mTOR pathway, which is activated by RTK-activating growth factors such as insulin, the IGFs and EGF, regulates many cellular responses; for instance, it enhances cell cycle turnover, leads to increased amounts of CREB (which increases hippocampal progenitor proliferation, for example), and upregulates astrocyte synthesis and storage of glycogen, cholesterol, and fatty acids. The increase of 28 RTKs, five NRTKs and 27 growth factors (Table S4), most of which peaked 24 h post-infusion when ketamine's antidepressant effect is also at its peak, demonstrates a continued ketamine interaction—as opposed to a return to homeostasis—and supports an overall "rewiring" of brain networks due to increased protein synthesis in conjunction with enhanced glial metabolism.[85]

Ketamine's antidepressant mechanism most likely does not result from a single molecular interaction. As we and others have suggested, one set of molecular interactions may drive the rapid antidepressant effect while others may be responsible for the days-to-weeks-long durability. Further, ketamine is extensively metabolized, and its metabolites have also been shown to be pharmacologically active. Consequently, the combination of ketamine and its metabolites may play separate roles in the rapid response and/or length of duration. In this exploratory study, we found that ketamine affects several pathways, likely resulting over time in neurogenesis and synaptic plasticity, and thereby improving the connectivity of functional circuits.

Limitations of the study

This study has severable notable limitations. First, the sample size was small, limiting the overall power of the study. Second, the participants were healthy volunteers, so correlating ketamine's and/or its metabolites' antidepressant effects with protein analysis was not possible. Third, although there are known sex-specific differences in the effects of ketamine,[114] differences between male and female participants could not be studied due to limited sample size, which may have made it more likely that pathways without sex-specific differences were identified. Fourth, there was no vehicle control group to compare CSF protein alterations as a factor of time with those that were altered following ketamine infusion. Future studies should seek to explore metabolomic and proteomic profiling in human CSF with larger sample sizes that will allow investigators to study differences between male and female participants and in patients with mood disorders in order to reveal potentially important biomarkers to assess neuropsychiatric diseases and help develop targeted antidepressant agents. Despite these limitations, this study clearly demonstrated for the first time that ketamine and its downstream metabolites cross the BBB. In addition, the exploratory analysis demonstrated clear proteomic changes resulting from the effects of ketamine and its metabolites in the CSF compartment,[24] lending insight into the relationship between these measures and protein expression levels.

STAR★METHODS

Detailed methods are provided in the online version of this paper and include the following:

SUPPLEMENTAL INFORMATION

Supplemental information can be found online at https://doi.org/10.1016/j.isci.2023.108527.

ACKNOWLEDGMENTS

Funding for this work was supported by the Intramural Research Programs of the National Institute on Aging, National Institutes of Health (ZIAAG000297) and the National Institute of Mental Health, National Institutes of Health (ZIAMH002857). The authors thank the 7SE research unit and staff for their support, Jacqueline Lovett for carrying out the bioanalysis of ketamine and metabolites in both the plasma and CSF samples, and Ioline Henter (NIMH) for invaluable editorial assistance.

AUTHOR CONTRIBUTIONS

RM and CAZ conceived and designed the experiment. MY, BK, EAD, PY, and LTP acquired and handled clinical samples. RM, MZ, JF, GF, QC, EL, and SD conducted experiments and/or acquired data. CAF carried out the data analysis. RM, JME, LF, and CAZ interpreted the data. RM, CAF, MY, JME, and CAZ designed and prepared the figures for the article. RM drafted the original article with critical review from CAF, MY, BK, TG, JME, LF, and CAZ. All authors reviewed and approved the final article. All authors agree to be accountable for all aspects of the work.

DECLARATION OF INTERESTS

Dr. Zarate is listed as a coinventor on a patent for the use of ketamine in major depression and suicidal ideation. Drs. Zarate and Moaddel are listed as coinventors on a patent for the use of (2*R*,6*R*)-hydroxynorketamine, (*S*)-dehydronorketamine, and other stereoisomeric dehydroxylated and hydroxylated metabolites of (*R*,*S*)-ketamine metabolites in the treatment of depression and neuropathic pain. Drs. Zarate, Moaddel, and Gould are listed as co-inventors on a patent application for the crystal forms and methods of synthesis of (2*R*,6*R*)-hydroxynorketamine and (2*S*,6*S*)-hydroxynorketamine and the use of (2*R*,6*R*)-hydroxynorketamine and (2*S*,6*S*)-hydroxynorketamine in the treatment of depression, anxiety, anhedonia, suicidal ideation, and post-traumatic stress disorders. Drs. Zarate and Moaddel have assigned their patent rights to the U.S. government but will share a percentage of any royalties that may be received by the government. Dr. Gould has assigned his patent rights to the University of Maryland. All other authors have no conflict of interest to disclose, financial or otherwise.

Clinical Trials Registration: NCT03065335.

Received: September 1, 2023
Revised: October 13, 2023
Accepted: November 20, 2023
Published: November 23, 2023

REFERENCES

1. Berman, R.M., Cappiello, A., Anand, A., Oren, D.A., Heninger, G.R., Charney, D.S., and Krystal, J.H. (2000). Antidepressant effects of ketamine in depressed patients. Biol. Psychiatry *47*, 351–354.
2. Diazgranados, N., Ibrahim, L., Brutsche, N.E., Newberg, A., Kronstein, P., Khalife, S., Kammerer, W.A., Quezado, Z., Luckenbaugh, D.A., Salvadore, G., et al. (2010). A randomized add-on trial of an N-methyl-D-aspartate antagonist in treatment-resistant bipolar depression. Arch. Gen. Psychiatry *67*, 793–802.
3. Zarate, C.A., Jr., Brutsche, N.E., Ibrahim, L., Franco-Chaves, J., Diazgranados, N., Cravchik, A., Selter, J., Marquardt, C.A., Liberty, V., and Luckenbaugh, D.A. (2012). Replication of ketamine's antidepressant efficacy in bipolar depression: a randomized controlled add-on trial. Biol. Psychiatry *71*, 939–946.
4. Fava, M., Freeman, M.P., Flynn, M., Judge, H., Hoeppner, B.B., Cusin, C., Ionescu, D.F., Mathew, S.J., Chang, L.C., Iosifescu, D.V., et al. (2020). Double-blind, placebo-controlled, dose-ranging trial of intravenous ketamine as adjunctive therapy in treatment-resistant depression (TRD). Mol. Psychiatry *25*, 1592–1603.
5. Murrough, J.W., Iosifescu, D.V., Chang, L.C., Al Jurdi, R.K., Green, C.E., Perez, A.M., Iqbal, S., Pillemer, S., Foulkes, A., Shah, A., et al. (2013). Antidepressant efficacy of ketamine in treatment-resistant major depression: a two-site randomized controlled trial. Am. J. Psychiatry *170*, 1134–1142.
6. Singh, J.B., Fedgchin, M., Daly, E.J., De Boer, P., Cooper, K., Lim, P., Pinter, C., Murrough, J.W., Sanacora, G., Shelton, R.C., et al. (2016). A double-blind, randomized, placebo-controlled, dose-frequency study of intravenous ketamine in patients with treatment-resistant depression. Am. J. Psychiatry *173*, 816–826.
7. Zarate, C.A., Jr., Singh, J.B., Carlson, P.J., Brutsche, N.E., Ameli, R., Luckenbaugh, D.A., Charney, D.S., and Manji, H.K. (2006). A randomized trial of an N-methyl-D-aspartate antagonist in treatment-resistant major depression. Arch. Gen. Psychiatry *63*, 856–864.
8. Zanos, P., Moaddel, R., Morris, P.J., Georgiou, P., Fischell, J., Elmer, G.I., Alkondon, M., Yuan, P., Pribut, H.J., Singh, N.S., et al. (2016). NMDAR inhibition-independent antidepressant actions of ketamine metabolites. Nature *533*, 481–486.
9. Maeng, S., Zarate, C.A., Jr., Du, J., Schloesser, R.J., McCammon, J., Chen, G., and Manji, H.K. (2008). Cellular mechanisms underlying the antidepressant effects of ketamine: role of alpha-amino-3-hydroxy-5-methylisoxazole-4-propionic acid receptors. Biol. Psychiatry *63*, 349–352.
10. Lener, M.S., Niciu, M.J., Ballard, E.D., Park, M., Park, L.T., Nugent, A.C., and Zarate, C.A., Jr. (2017). Glutamate and gamma-aminobutyric acid systems in the pathophysiology of major depression and antidepressant response to ketamine. Biol. Psychiatry *81*, 886–897.
11. Niesters, M., Martini, C., and Dahan, A. (2014). Ketamine for chronic pain: risks and benefits. Br. J. Clin. Pharmacol. *77*, 357–367.
12. Schwartzman, R.J., Alexander, G.M., Grothusen, J.R., Paylor, T., Reichenberger, E., and Perreault, M. (2009). Outpatient intravenous ketamine for the treatment of complex regional pain syndrome: a double-blind placebo controlled study. Pain *147*, 107–115.
13. Moaddel, R., Venkata, S.L.V., Tanga, M.J., Bupp, J.E., Green, C.E., Iyer, L., Furimsky, A., Goldberg, M.E., Torjman, M.C., and Wainer, I.W. (2010). A parallel chiral-achiral liquid chromatographic method for the determination of the stereoisomers of ketamine and ketamine metabolites in the plasma and urine of patients with complex regional pain syndrome. Talanta *82*, 1892–1904.
14. Farmer, C.A., Gilbert, J.R., Moaddel, R., George, J., Adeojo, L., Lovett, J., Nugent, A.C., Kadriu, B., Yuan, P.X., Gould, T.D., et al. (2020). Ketamine metabolites, clinical response, and gamma power in a randomized, placebo-controlled, crossover trial for treatment-resistant major depression (vol 45, pg 861, 2020). Neuropsychopharmacology *45*, 1405.
15. Gould, T.D., Zanos, P., and Zarate, C.A., Jr. (2017). Ketamine mechanism of action: separating the wheat from the chaff. Neuropsychopharmacology *42*, 368–369.
16. Rao, L.K., Flaker, A.M., Friedel, C.C., and Kharasch, E.D. (2016). Role of cytochrome P4502B6 polymorphisms in ketamine metabolism and clearance. Anesthesiology *125*, 1103–1112.
17. Desta, Z., Moaddel, R., Ogburn, E.T., Xu, C., Ramamoorthy, A., Venkata, S.L.V., Sanghvi, M., Goldberg, M.E., Torjman, M.C., and Wainer, I.W. (2012). Stereoselective and regiospecific hydroxylation of ketamine and norketamine. Xenobiotica *42*, 1076–1087.
18. Chou, D., Peng, H.Y., Lin, T.B., Lai, C.Y., Hsieh, M.C., Wen, Y.C., Lee, A.S., Wang, H.H., Yang, P.S., Chen, G.D., and Ho, Y.C. (2018). (2R,6R)-hydroxynorketamine rescues chronic stress-induced depression-like behavior through its actions in the midbrain periaqueductal gray. Neuropharmacology *139*, 1–12.
19. Pham, T.H., Defaix, C., Xu, X., Deng, S.X., Fabresse, N., Alvarez, J.C., Landry, D.W., Brachman, R.A., Denny, C.A., and Gardier, A.M. (2018). Common neurotransmission recruited in (R,S)-ketamine and (2R,6R)-hydroxynorketamine-induced sustained antidepressant-like effects. Biol. Psychiatry *84*, e3–e6.
20. Zarate, C.A., Brutsche, N., Laje, G., Luckenbaugh, D.A., Venkata, S.L.V., Ramamoorthy, A., Moaddel, R., and Wainer, I.W. (2012). Relationship of Ketamine's Plasma Metabolites with Response, Diagnosis, and Side Effects in Major Depression. Biol Psychiat *72*, 331–338.
21. Zhao, X., Venkata, S.L.V., Moaddel, R., Luckenbaugh, D.A., Brutsche, N.E., Ibrahim, L., Zarate, C.A., Mager, D.E., and Wainer, I.W. (2012). Simultaneous population pharmacokinetic modelling of ketamine and three major metabolites in patients with treatment-resistant bipolar depression. Br. J. Clin. Pharmacol. *74*, 304–314.
22. Zanos, P., and Gould, T.D. (2018). Mechanisms of ketamine action as an antidepressant. Mol. Psychiatry *23*, 801–811.
23. Santos, J., Milthorpe, B.K., and Padula, M.P. (2019). Proteomic Analysis of Cyclic Ketamine Compounds Ability to Induce Neural Differentiation in Human Adult Mesenchymal Stem Cells. Int. J. Mol. Sci. *20*, 523.
24. Moaddel, R., Zanos, P., Farmer, C.A., Kadriu, B., Morris, P.J., Lovett, J., Acevedo-Diaz, E.E., Cavanaugh, G.W., Yuan, P., Yavi, M., et al. (2022). Comparative metabolomic analysis in plasma and cerebrospinal fluid of humans and in plasma and brain of mice following antidepressant-dose ketamine administration. Transl Psychiat *12*, 179.
25. Moaddel, R., Sanghvi, M., Dossou, K.S.S., Ramamoorthy, A., Green, C., Bupp, J., Swezey, R., O'Loughlin, K., and Wainer, I.W. (2015). The distribution and clearance of (2S,6S)-hydroxynorketamine, an active ketamine metabolite, in Wistar rats. Pharmacol Res Perspe *3*, e00157.
26. Highland, J.N., Morris, P.J., Konrath, K.M., Riggs, L.M., Hagen, N.R., Zanos, P., Powels, C.F., Moaddel, R., Thomas, C.J., Wang, A.Q., and Gould, T.D. (2022). Hydroxynorketamine Pharmacokinetics and Antidepressant Behavioral Effects of (2,6)- and (5R)-Methyl-(2R,6R)-hydroxynorketamines. ACS Chem. Neurosci. *13*, 510–523.
27. Kamp, J., Jonkman, K., van Velzen, M., Aarts, L., Niesters, M., Dahan, A., and Olofsen, E. (2020). Pharmacokinetics of ketamine and its major metabolites norketamine, hydroxynorketamine, and dehydronorketamine: a model-based analysis. Br. J. Anaesth. *125*, 750–761.
28. Schittenhelm, L., Hilkens, C.M., and Morrison, V.L. (2017). beta(2) Integrins As Regulators of Dendritic Cell, Monocyte, and Macrophage Function. Front. Immunol. *8*, 1866.
29. Sajjadi, S.S., Foshati, S., Haddadian-Khouzani, S., and Rouhani, M.H. (2022). The role of selenium in depression: a systematic review and meta-analysis of human observational and interventional studies. Sci. Rep. *12*, 1045.
30. Seale, L.A., Hashimoto, A.C., Kurokawa, S., Gilman, C.L., Seyedali, A., Bellinger, F.P., Raman, A.V., and Berry, M.J. (2012). Disruption of the selenocysteine lyase-mediated selenium recycling pathway leads to metabolic syndrome in mice. Mol. Cell Biol. *32*, 4141–4154.
31. Liu, J.R., Baek, C., Han, X.H., Shoureshi, P., and Soriano, S.G. (2013). Role of glycogen synthase kinase-3beta in ketamine-induced developmental neuroapoptosis in rats. Br. J. Anaesth. *110*, i3–i9.
32. Aguilar-Valles, A., De Gregorio, D., Matta-Camacho, E., Eslamizade, M.J., Khlaifia, A., Skaleka, A., Lopez-Canul, M., Torres-Berrio, A., Bermudez, S., Rurak, G.M., et al. (2021). Antidepressant actions of ketamine engage cell-specific translation via eIF4E. Nature *590*, 315–319.
33. Robaczewska, J., Kędziora-Kornatowska, K., Kucharski, R., Nowak, M., Muszalik, M., Kornatowski, M., and Kędziora, J. (2016). Decreased expression of heme oxygenase is associated with depressive symptoms and may contribute to depressive and hypertensive comorbidity. Redox Rep. *21*, 209–218.
34. Israel-Elgali, I., Hertzberg, L., Shapira, G., Segev, A., Krieger, I., Nitzan, U., Bloch, Y., Pillar, N., Mayer, O., Weizman, A., et al. (2021). Blood transcriptional response to treatment-resistant depression during

electroconvulsive therapy. J. Psychiatr. Res. *141*, 92–103.
35. Takahashi, K., Kurokawa, K., Hong, L., Miyagawa, K., Mochida-Saito, A., Iwasa, M., Iwasa, H., Nakagawasai, O., Tadano, T., Takeda, H., and Tsuji, M. (2022). Antidepressant effects of Enterococcus faecalis 2001 through the regulation of prefrontal cortical myelination via the enhancement of CREB/BDNF and NF-KB p65/LIF/STAT3 pathways in olfactory bulbectomized mice. J. Psychiatr. Res. *148*, 137–148.
36. Yücel, D. (2022). Ketamine induces apical extracellular matrix modifications in Caenorhabditis elegans. Sci. Rep. *12*, 22122.
37. Liu, W., Zheng, Y., Zhang, F., Zhu, M., Guo, Q., Xu, H., Liu, C., Chen, H., Wang, X., Hu, Y., et al. (2021). A Preliminary Investigation on Plasma Cell Adhesion Molecules Levels by Protein Microarray Technology in Major Depressive Disorder. Front. Psychiatry *12*, 627469.
38. Al Shweiki, M.R., Oeckl, P., Steinacker, P., Barschke, P., Dorner-Ciossek, C., Hengerer, B., Schönfeldt-Lecuona, C., and Otto, M. (2020). Proteomic analysis reveals a biosignature of decreased synaptic protein in cerebrospinal fluid of major depressive disorder. Transl. Psychiatry *10*, 144.
39. Schnell, U., Cirulli, V., and Giepmans, B.N.G. (2013). EpCAM: structure and function in health and disease. Biochim. Biophys. Acta *1828*, 1989–2001.
40. Zhao, P., Xu, Y., Jiang, L.L., Fan, X., Ku, Z., Li, L., Liu, X., Deng, M., Arase, H., Zhu, J.J., et al. (2022). LILRB2-mediated TREM2 signaling inhibition suppresses microglia functions. Mol. Neurodegener. *17*, 44.
41. Samaniego, R., Dominguez-Soto, A., Ratnam, M., Matsuyama, T., Sanchez-Mateos, P., Corbi, A.L., and Puig-Kroger, A. (2020). Folate Receptor beta (FRbeta) Expression in Tissue-Resident and Tumor-Associated Macrophages Associates with and Depends on the Expression of PU.1. Cells *9*, 1445.
42. Alcaraz, M.J., Fernández, P., and Guillén, M.I. (2003). Anti-inflammatory actions of the heme oxygenase-1 pathway. Curr. Pharm. Des. *9*, 2541–2551.
43. Moaddel, R., Shardell, M., Khadeer, M., Lovett, J., Kadriu, B., Ravichandran, S., Morris, P.J., Yuan, P., Thomas, C.J., Gould, T.D., et al. (2018). Plasma metabolomic profiling of a ketamine and placebo crossover trial of major depressive disorder and healthy control subjects. Psychopharmacology *235*, 3017–3030.
44. Kadriu, B., Farmer, C.A., Yuan, P., Park, L.T., Deng, Z.D., Moaddel, R., Henter, I.D., Shovestul, B., Ballard, E.D., Kraus, C., et al. (2021). The kynurenine pathway and bipolar disorder: intersection of the monoaminergic and glutamatergic systems and immune response. Mol. Psychiatry *26*, 4085–4095.
45. Salustri, C., Tecchio, F., Zappasodi, F., Bevacqua, G., Fontana, M., Ercolani, M., Milazzo, D., Squitti, R., and Rossini, P.M. (2007). Cortical excitability and rest activity properties in patients with depression. J. Psychiatry Neurosci. *32*, 259–266.
46. Ren, W., Lou, H., Ren, X., Wen, G., Wu, X., Xia, X., Wang, S., Yu, X., Yan, L., Zhang, G., et al. (2022). Ketamine promotes the amyloidogenic pathway by regulating endosomal pH. Toxicology *471*, 153163.
47. Li, B., Yang, W., Ge, T., Wang, Y., and Cui, R. (2022). Stress induced microglial activation contributes to depression. Pharmacol. Res. *179*, 106145.
48. Hu, X., Li, S., Doycheva, D.M., Huang, L., Lenahan, C., Liu, R., Huang, J., Xie, S., Tang, J., Zuo, G., and Zhang, J.H. (2020). Rh-CSF1 attenuates neuroinflammation via the CSF1R/PLCG2/PKCepsilon pathway in a rat model of neonatal HIE. J. Neuroinflammation *17*, 182.
49. Sanchez-Ramos, J., Song, S., Cao, C., and Arendash, G. (2008). The potential of hematopoietic growth factors for treatment of Alzheimer's disease: a mini-review. BMC Neurosci. *9*, S3.
50. Prieto, G.A., and Cotman, C.W. (2017). Cytokines and cytokine networks target neurons to modulate long-term potentiation. Cytokine Growth Factor Rev. *34*, 27–33.
51. Matutino Santos, P., Pereira Campos, G., and Nascimento, C. (2023). Endo-Lysosomal and Autophagy Pathway and Ubiquitin-Proteasome System in Mood Disorders: A Review Article. Neuropsychiatr. Dis. Treat. *19*, 133–151.
52. Poggetti, V., Salerno, S., Baglini, E., Barresi, E., Da Settimo, F., and Taliani, S. (2022). Carbonic Anhydrase Activators for Neurodegeneration: An Overview. Molecules *27*, 2544.
53. Nuriel, T., Peng, K.Y., Ashok, A., Dillman, A.A., Figueroa, H.Y., Apuzzo, J., Ambat, J., Levy, E., Cookson, M.R., Mathews, P.M., and Duff, K.E. (2017). The Endosomal-Lysosomal Pathway Is Dysregulated by APOE4 Expression in Vivo. Front. Neurosci. *11*, 702.
54. Chen, D.T.L., Cheng, S.W., Chen, T., Chang, J.P.C., Hwang, B.F., Chang, H.H., Chuang, E.Y., Chen, C.H., and Su, K.P. (2022). Identification of Genetic Variations in the NAD-Related Pathways for Patients with Major Depressive Disorder: A Case-Control Study in Taiwan. J. Clin. Med. *11*, 3622.
55. Walker, K.A., Basisty, N., Wilson, D.M., 3rd, and Ferrucci, L. (2022). Connecting aging biology and inflammation in the omics era. J. Clin. Invest. *132*, e158448.
56. Penna, E., Cerciello, A., Chambery, A., Russo, R., Cernilogar, F.M., Pedone, E.M., Perrone-Capano, C., Cappello, S., Di Giaimo, R., and Crispino, M. (2019). Cystatin B Involvement in Synapse Physiology of Rodent Brains and Human Cerebral Organoids. Front. Mol. Neurosci. *12*, 195.
57. Beydoun, M.A., Beydoun, H.A., Boueiz, A., Shroff, M.R., and Zonderman, A.B. (2013). Antioxidant status and its association with elevated depressive symptoms among US adults: National Health and Nutrition Examination Surveys 2005-6. Br. J. Nutr. *109*, 1714–1729.
58. Blaner, W.S., Brun, P.J., Calderon, R.M., and Golczak, M. (2020). Retinol-binding protein 2 (RBP2): biology and pathobiology. Crit. Rev. Biochem. Mol. Biol. *55*, 197–218.
59. Bai, H., Yang, B., Yu, W., Xiao, Y., Yu, D., and Zhang, Q. (2018). Cathepsin B links oxidative stress to the activation of NLRP3 inflammasome. Exp. Cell Res. *362*, 180–187.
60. Niemeyer, C., Matosin, N., Kaul, D., Philipsen, A., and Gassen, N.C. (2020). The Role of Cathepsins in Memory Functions and the Pathophysiology of Psychiatric Disorders. Front. Psychiatry *11*, 718.
61. Nixon, R.A. (2020). The aging lysosome: An essential catalyst for late-onset neurodegenerative diseases. Bba-Proteins Proteom *1868*, 140443.
62. Wang, F., Salvati, A., and Boya, P. (2018). Lysosome-dependent cell death and deregulated autophagy induced by amine-modified polystyrene nanoparticles. Open Biol. *8*, 170271.
63. Gonzalez, A., Valeiras, M., Sidransky, E., and Tayebi, N. (2014). Lysosomal integral membrane protein-2: a new player in lysosome-related pathology. Mol. Genet. Metab. *111*, 84–91.
64. Rothaug, M., Zunke, F., Mazzulli, J.R., Schweizer, M., Altmeppen, H., Lüllmann-Rauch, R., Kallemeijn, W.W., Gaspar, P., Aerts, J.M., Glatzel, M., et al. (2014). LIMP-2 expression is critical for beta-glucocerebrosidase activity and alpha-synuclein clearance. Proc. Natl. Acad. Sci. USA *111*, 15573–15578.
65. Gamp, A.C., Tanaka, Y., Lüllmann-Rauch, R., Wittke, D., D'Hooge, R., De Deyn, P.P., Moser, T., Maier, H., Hartmann, D., Reiss, K., et al. (2003). LIMP-2/LGP85 deficiency causes ureteric pelvic junction obstruction, deafness and peripheral neuropathy in mice. Hum. Mol. Genet. *12*, 631–646.
66. Yim, W.W.Y., and Mizushima, N. (2020). Lysosome biology in autophagy. Cell Discov. *6*, 6.
67. Fries, G.R., Saldana, V.A., Finnstein, J., and Rein, T. (2023). Molecular pathways of major depressive disorder converge on the synapse. Mol. Psychiatry *28*, 284–297.
68. Jensen, G.S., Leon-Palmer, N.E., and Townsend, K.L. (2021). Bone morphogenetic proteins (BMPs) in the central regulation of energy balance and adult neural plasticity. Metabolism *123*, 154837.
69. Kékesi, K.A., Juhász, G., Simor, A., Gulyássy, P., Szegő, E.M., Hunyadi-Gulyás, E., Darula, Z., Medzihradszky, K.F., Palkovits, M., Penke, B., and Czurkó, A. (2012). Altered functional protein networks in the prefrontal cortex and amygdala of victims of suicide. PLoS One *7*, e50532.
70. Weckmann, K., Deery, M.J., Howard, J.A., Feret, R., Asara, J.M., Dethloff, F., Filiou, M.D., Iannace, J., Labermaier, C., Maccarrone, G., et al. (2017). Ketamine's antidepressant effect is mediated by energy metabolism and antioxidant defense system. Sci. Rep. *7*, 15788.
71. Shurubor, Y.I., Cooper, A.J.L., Krasnikov, A.B., Isakova, E.P., Deryabina, Y.I., Beal, M.F., and Krasnikov, B.F. (2020). Changes of Coenzyme A and Acetyl-Coenzyme A Concentrations in Rats after a Single-Dose Intraperitoneal Injection of Hepatotoxic Thioacetamide Are Not Consistent with Rapid Recovery. Int. J. Mol. Sci. *21*, 8918.
72. Park, J., van Koeverden, P., Singh, B., and Gupta, R.S. (2007). Identification and characterization of human ribokinase and comparison of its properties with E. coli ribokinase and human adenosine kinase. FEBS Lett. *581*, 3211–3216.
73. Weckmann, K., Labermaier, C., Asara, J.M., Müller, M.B., and Turck, C.W. (2014). Time-dependent metabolomic profiling of Ketamine drug action reveals hippocampal pathway alterations and biomarker candidates. Transl. Psychiatry *4*, e481.
74. Cheffer, A., Castillo, A.R.G., Corrêa-Velloso, J., Gonçalves, M.C.B., Naaldijk, Y., Nascimento, I.C., Burnstock, G., and Ulrich, H. (2018). Purinergic system in psychiatric diseases. Mol. Psychiatry *23*, 94–106.
75. Zimmermann, H. (2021). Ectonucleoside triphosphate diphosphohydrolases and ecto-5'-nucleotidase in purinergic

signaling: how the field developed and where we are now. Purinergic Signal. *17*, 117–125.
76. Bao, X.R., Ong, S.E., Goldberger, O., Peng, J., Sharma, R., Thompson, D.A., Vafai, S.B., Cox, A.G., Marutani, E., Ichinose, F., et al. (2016). Mitochondrial dysfunction remodels one-carbon metabolism in human cells. Elife *5*, e10575.
77. Minelli, A., Magri, C., Barbon, A., Bonvicini, C., Segala, M., Congiu, C., Bignotti, S., Milanesi, E., Trabucchi, L., Cattane, N., et al. (2015). Proteasome system dysregulation and treatment resistance mechanisms in major depressive disorder. Transl Psychiat *5*, e687.
78. Distler, M.G., and Palmer, A.A. (2012). Role of Glyoxalase 1 (Glo1) and methylglyoxal (MG) in behavior: recent advances and mechanistic insights. Front. Genet. *3*, 250.
79. Wang, J.Q., Derges, J.D., Bodepudi, A., Pokala, N., and Mao, L.M. (2022). Roles of non-receptor tyrosine kinases in pathogenesis and treatment of depression. J. Integr. Neurosci. *21*, 25.
80. Qiu, S., Lu, Z., and Levitt, P. (2014). MET receptor tyrosine kinase controls dendritic complexity, spine morphogenesis, and glutamatergic synapse maturation in the hippocampus. J. Neurosci. *34*, 16166–16179.
81. Wintheiser, G.A., and Silberstein, P. (2022). Physiology, Tyrosine Kinase Receptors (StatPearls).
82. Cheng, Y., Sun, M., Wang, F., Geng, X., and Wang, F. (2021). Identification of Hub Genes Related to Alzheimer's Disease and Major Depressive Disorder. Am. J. Alzheimers Dis. Other Demen. *36*, 15333175211046123.
83. Nugent, A.C., Ballard, E.D., Gould, T.D., Park, L.T., Moaddel, R., Brutsche, N.E., and Zarate, C.A., Jr. (2019). Ketamine has distinct electrophysiological and behavioral effects in depressed and healthy subjects. Mol. Psychiatry *24*, 1040–1052.
84. Romano, R., and Bucci, C. (2020). Role of EGFR in the Nervous System. Cells *9*, 1887.
85. Kavalali, E.T., and Monteggia, L.M. (2015). How does ketamine elicit a rapid antidepressant response? Curr. Opin. Pharmacol. *20*, 35–39.
86. Mazucanti, C.H., Liu, Q.R., Lang, D., Huang, N., O'Connell, J.F., Camandola, S., and Egan, J.M. (2019). Release of insulin produced by the choroid plexis is regulated by serotonergic signaling. Jci Insight *4*, e131682.
87. Ma, Z.Y., Chen, F., Xiao, P., Zhang, X.M., and Gao, X.X. (2019). Silence of MiR-9 protects depression mice through Notch signaling pathway. Eur Rev Med Pharmaco *23*, 4961–4970.
88. Shi, Y., Li, J., Chen, C., Xia, Y., Li, Y., Zhang, P., Xu, Y., Li, T., Zhou, W., and Song, W. (2018). Ketamine Modulates Zic5 Expression via the Notch Signaling Pathway in Neural Crest Induction. Front. Mol. Neurosci. *11*, 9.
89. LaFoya, B., Munroe, J.A., Mia, M.M., Detweiler, M.A., Crow, J.J., Wood, T., Roth, S., Sharma, B., and Albig, A.R. (2016). Notch: A multi-functional integrating system of microenvironmental signals. Dev. Biol. *418*, 227–241.
90. Pollerberg, G.E., Thelen, K., Theiss, M.O., and Hochlehnert, B.C. (2013). The role of cell adhesion molecules for navigating axons: density matters. Mech. Dev. *130*, 359–372.
91. Meltzer, H., and Schuldiner, O. (2022). Spatiotemporal Control of Neuronal Remodeling by Cell Adhesion Molecules: Insights From Drosophila. Front. Neurosci. *16*, 897706.
92. Fujioka, H., Dairyo, Y., Yasunaga, K.I., and Emoto, K. (2012). Neural functions of matrix metalloproteinases: plasticity, neurogenesis, and disease. Biochem. Res. Int. *2012*, 789083.
93. Shrestha, B.R., Burgos, A., and Grueber, W.B. (2021). The Immunoglobulin Superfamily Member Basigin Is Required for Complex Dendrite Formation in Drosophila. Front. Cell. Neurosci. *15*, 739741.
94. Mao, L.M., and Wang, J.Q. (2020). Linkage of Non-receptor Tyrosine Kinase Fyn to mGlu5 Receptors in Striatal Neurons in a Depression Model. Neuroscience *433*, 11–20.
95. Matrone, C., Petrillo, F., Nasso, R., and Ferretti, G. (2020). Fyn Tyrosine Kinase as Harmonizing Factor in Neuronal Functions and Dysfunctions. Int. J. Mol. Sci. *21*, 4444.
96. Magdaleno, S.M., and Curran, T. (2001). Brain development: Integrins and the Reelin pathway. Curr. Biol. *11*, R1032–R1035.
97. Kim, J.W., Herz, J., Kavalali, E.T., and Monteggia, L.M. (2021). A key requirement for synaptic Reelin signaling in ketamine-mediated behavioral and synaptic action. Proc. Natl. Acad. Sci. USA *118*, e2103079118.
98. Hethorn, W.R., Ciarlone, S.L., Filonova, I., Rogers, J.T., Aguirre, D., Ramirez, R.A., Grieco, J.C., Peters, M.M., Gulick, D., Anderson, A.E., et al. (2015). Reelin supplementation recovers synaptic plasticity and cognitive deficits in a mouse model for Angelman syndrome. Eur. J. Neurosci. *41*, 1372–1380.
99. Birge, R.B., Kalodimos, C., Inagaki, F., and Tanaka, S. (2009). Crk and CrkL adaptor proteins: networks for physiological and pathological signaling. Cell Commun. Signal. *7*, 13.
100. Ishii, K., Kubo, K.I., and Nakajima, K. (2016). Reelin and Neuropsychiatric Disorders. Front. Cell. Neurosci. *10*, 229.
101. Diaz, A., Martin-Jimenez, C., Woo, Y., Merino, P., Torre, E., and Yepes, M. (2022). Urokinase-Type Plasminogen Activator Triggers Wingless/Int1-Independent Phosphorylation of the Low-Density Lipoprotein Receptor-Related Protein-6 in Cerebral Cortical Neurons. J. Alzheimers Dis. *89*, 877–891.
102. Gambella, A., Senetta, R., Collemi, G., Vallero, S.G., Monticelli, M., Cofano, F., Zeppa, P., Garbossa, D., Pellerino, A., Rudà, R., et al. (2020). NTRK Fusions in Central Nervous System Tumors: A Rare, but Worthy Target. Int. J. Mol. Sci. *21*, 753.
103. Funa, K., and Sasahara, M. (2014). The roles of PDGF in development and during neurogenesis in the normal and diseased nervous system. J. Neuroimmune Pharmacol. *9*, 168–181.
104. Sil, S., Periyasamy, P., Thangaraj, A., Chivero, E.T., and Buch, S. (2018). PDGF/PDGFR axis in the neural systems. Mol. Aspects Med. *62*, 63–74.
105. Spinelli, M., Fusco, S., and Grassi, C. (2019). Brain Insulin Resistance and Hippocampal Plasticity: Mechanisms and Biomarkers of Cognitive Decline. Front. Neurosci. *13*, 788.
106. Fitzgerald, P.J., and Watson, B.O. (2018). Gamma oscillations as a biomarker for major depression: an emerging topic. Transl Psychiat *8*, 177.
107. Adaikkan, C., Middleton, S.J., Marco, A., Pao, P.C., Mathys, H., Kim, D.N.W., Gao, F., Young, J.Z., Suk, H.J., Boyden, E.S., et al. (2019). Gamma Entrainment Binds Higher-Order Brain Regions and Offers Neuroprotection. Neuron *102*, 929–943.e8.
108. Vico Varela, E., Etter, G., and Williams, S. (2019). Excitatory-inhibitory imbalance in Alzheimer's disease and therapeutic significance. Neurobiol. Dis. *127*, 605–615.
109. Darwish, L., Beroncal, E., Sison, M.V., and Swardfager, W. (2018). Depression in people with type 2 diabetes: current perspectives. Diabetes Metab. Syndr. Obes. *11*, 333–343.
110. Price, J.B., Yates, C.G., Morath, B.A., van de Wakker, S.K., Yates, N.J., Butters, K., Frye, M.A., McGee, S.L., and Tye, S.J. (2021). Lithium augmentation of ketamine increases insulin signaling and antidepressant-like active stress coping in a rodent model of treatment-resistant depression. Transl Psychiat *11*, 598.
111. Cai, W., Xue, C., Sakaguchi, M., Konishi, M., Shirazian, A., Ferris, H.A., Li, M.E., Yu, R., Kleinridders, A., Pothos, E.N., and Kahn, C.R. (2018). Insulin regulates astrocyte gliotransmission and modulates behavior. J. Clin. Invest. *128*, 2914–2926.
112. Pham, T.H., and Gardier, A.M. (2019). Fast-acting antidepressant activity of ketamine: highlights on brain serotonin, glutamate, and GABA neurotransmission in preclinical studies. Pharmacol. Ther. *199*, 58–90.
113. Laplante, M., and Sabatini, D.M. (2013). Regulation of mTORC1 and its impact on gene expression at a glance. J. Cell Sci. *126*, 1713–1719.
114. Ponton, E., Turecki, G., and Nagy, C. (2022). Sex Differences in the Behavioral, Molecular, and Structural Effects of Ketamine Treatment in Depression. Int. J. Neuropsychopharmacol. *25*, 75–84.
115. Hasan, M., Hofstetter, R., Fassauer, G.M., Link, A., Siegmund, W., and Oswald, S. (2017). Quantitative chiral and achiral determination of ketamine and its metabolites by LC–MS/MS in human serum, urine and fecal samples. J. Pharm. Biomed. Anal. *139*, 87–97.
116. Assarsson, E., Lundberg, M., Holmquist, G., Björkesten, J., Thorsen, S.B., Ekman, D., Eriksson, A., Rennel Dickens, E., Ohlsson, S., Edfeldt, G., et al. (2014). Homogenous 96-plex PEA immunoassay exhibiting high sensitivity, specificity, and excellent scalability. PLoS One *9*, e95192.
117. Wasserstein, R.L., Schirm, A.L., and Lazar, N.A. (2019). Moving to a World Beyond "p < 0.05". Am. Stat. *73*, 1–19.
118. Jaki, T., and Wolfsegger, M.J. (2011). Estimation of pharmacokinetic parameters with the R package PK. Pharm. Stat. *10*, 284–288.
119. Bates, D., Mächler, M., Bolker, B., and Walker, S. (2015). Fitting Linear Mixed-Effects Models Using lme4. J. Stat. Softw. *67*, 1–48.

STAR★METHODS

KEY RESOURCES TABLE

REAGENT or RESOURCE	SOURCE	IDENTIFIER
Chemicals, peptides, and recombinant proteins		
ammonium acetate	Sigma	A1542
acetonitrile, LC-MS grade	Sigma	AX0156-1
isopropanol, Lc-MS grade	Sigma	1027814000
(2*R*,6*R*)-HNK	Tocris	6094
(2S,6S)-HNK	Tocris	6095
(*R*)-NK	Tocris	5996
(*S*)-NK	Tocris	6112
Ketamine	Cerilliant	K-002
Ketamine -d4 HCl	Cerilliant	K-006
Norketamine-d4	Cerilliant	N-037
Critical commercial assays		
Mercodia ultrasensitive insulin ELISA kit	Mercodia	10-1132-01
Olink Explore 384 Inflammation I Reagent Kit	Olink Proteomics	91101
Olink Explore 384 Oncology I Reagent Kit	Olink Proteomics	91102
Olink Explore 384 Cardiometabolic I Reagent Kit	Olink Proteomics	91103
Olink Explore Neurology I Reagent Kit	Olink Proteomics	91104
Software and algorithms		
PK version 1.3.5, package for R	Jaki T, Wolfsegger MJ. Estimation of pharmacokinetic parameters with the R package PK. Pharm Stat. 2011; 10(3):284-8.	NA
lme4 version 1.1.33, package for R	Bates D, Machler M, Bolker BM, Walker SC. Fitting Linear Mixed-Effects Models Using lme4. J Stat Softw. 2015; 67(1):1-48	NA
R version 4.3.0	R Core Team (2023). R: A Language and Environment for Statistical Computing. R Foundation for Statistical Computing, Vienna, Austria	
Other		
Eclipse XDB-C18 guard column (4.6 mm × 12.5 mm)	Agilent	820950–925
Lux® Amylose-2, LC Column (150 × 4.6 mm, 3um)	Phenomenex	00F-4471-EO
Varian Pursuit XRs 5 C18 (250 × 4.0 mm ID, 5 μm)	Agilent	A6000250X040
NovaSeq 6000 SP Reagent Kit v 1.5 (100 cycles),	Illumina	20028401

RESOURCE AVAILABILITY

Lead contact

Further information and requests should be directed to the Lead Contact, Ruin Moaddel (moaddelru@mail.nih.gov).

Materials availability

This study did not generate new unique reagents.

Data and code availability

The data used to generate all analyses reported in this manuscript are available from the lead contact upon request.

The R code used to generate all analyses reported in this manuscript are available from the lead contact upon request.

Any additional information required to reanalyze the data reported in this paper is available from the lead contact upon request. The data are not publicly available due to privacy or ethical restrictions.

EXPERIMENTAL MODEL AND STUDY PARTICIPANT DETAILS

Participants

All participants provided written consent prior to study entry, and this study was approved by the Combined Neuroscience Institutional Review Board of the NIH (NCT03065335); CONSORT details can be found in Figure 1. Nine healthy human volunteers aged 19–36 years (mean age = 27 ± 6; F:M 4:5; 4 White, 2 Black, 1 Asian, 1 multiple races) (Table S1) received a ketamine infusion (0.5 mg/kg/IV over 40 min) (Mylan Institutional, Galway, Ireland) and contributed plasma and CSF samples for up to 28 h. An intrathecal catheter was inserted via lumbar puncture in the operating room following aseptic practices approximately 6 h prior to ketamine infusion, thereby allowing for repeated collection of CSF (2–3 cc per sample). Whole blood and CSF were both collected at baseline (pre-infusion), at 40, 120, and 230 min post-infusion, and at 6, 10, 12, 22, 24, 26, and 28 h post-infusion, as previously described.[24] An additional blood sample was also collected at 48 h post-infusion. The blood was collected into heparinized BD vacutainer tubes that were then centrifuged at 3000 rpm at 4°C for 10 min; separated plasma samples were aliquoted and stored along with CSF at −80°C until assay.

METHOD DETAILS

Ketamine and metabolite measurements

CSF and plasma concentrations of ketamine, NK, and HNKs were measured using high-performance liquid chromatography-mass spectrometry (HPLC-MS), as previously described,[14] accomplished using an Eclipse XDB-C18 guard column (4.6 mm × 12.5 mm) and an analytical column Varian Pursuit XRs 5 C18 (250 × 4.0 mm ID, 5 μm). The mobile phase consisted of ammonium acetate [5 mM, pH 7.6] as Component A and acetonitrile as component B. A linear gradient was run as follows: 0 min 20% B; 5 min 20% B; 15 min 80% B; 20 min 20% B at a flow rate of 0.4 mL/min. The total run time was 30 min per sample. Resolution of (2*R*,6*R*)-HNK, (2*S*,6*S*)-HNK, (*R*)-NK, and (*S*)-NK was achieved via a previously described method with slight modifications.[115] Briefly, 200 μL plasma, 25 μL internal standard (50 ng/mL D4-K), and 25 μL water were added, and the samples were centrifuged for 10 min and extracted using solid phase extraction cartridges (Oasis HLB, Water Corp). After elution, the metabolites were stream-dried under nitrogen and reconstituted in 100 μL 0.1% formic acid in 90:10 methanol:water and transferred to autosampler vials for analysis. Separation of the metabolites was accomplished by a linear gradient over 35 min at a flow rate of 0.35 mL/min: 0–20 min 30% B, 20–22 min 70% B, 22–28 min 85% B, 28.1 min 30% B, 28.1–35 min at 30% B, on a Lux Amylose-2, LC Column (150 × 4.6 mm, 3 um, Phenomenex, Torrance, CA) at 40°C, with mobile phase A consisting of ammonium acetate (5 mM, pH 9) and mobile phase B consisting of isopropanol and acetonitrile (4:1). AUC was calculated for the enantiomers of NK and HNK by multiplying the observed NK or HNK concentration by the given proportion and calculating AUC as described above. Observed values were plotted. The data were log transformed after imputation but prior to analysis. The chiral data, which were proportions, are the exception.

Data were acquired using a Nexera XR HPLC (Shimadzu, Kyoto, Japan) coupled with a QTRAP 5500 (SCIEX) and analyzed with Analyst 1.6 (SCIEX). The positive ion mode was obtained using multiple reaction monitoring. The instrumental source setting for curtain gas, ion spray voltage, temperature, ion source gas 1, and ion source gas 2 were 25 psi, 5500 V, 400 C, 70 psi, and 40 psi, respectively. The collision-activated dissociation was set to medium, and the entrance potential was 10 V.

Proximity extension assay proteomic analysis

Proteins were measured using Olink Explore [1536] (Olink Proteomics AB, Uppsala, Sweden) according to the manufacturer's instructions. The technology behind the Olink protocol is based on Proximity Extension Assay (PEA),[116] coupled with readout via next-generation sequencing (NGS). The assay enables the detection of up to 1536 proteins in 90 samples simultaneously, using only 2.8 μL of CSF sample. A list of all proteins with the corresponding UniProt ID is provided in Table S5. In brief, pairs of oligonucleotide-labeled antibody probes designed for each protein bind to their target, bringing the complementary oligonucleotides in close proximity and allowing for their hybridization. The addition of a DNA polymerase leads to the extension of the hybridized oligonucleotides, generating a unique protein identification "barcode". Next, library preparation adds sample identification indexes and the required nucleotides for Illumina sequencing. Prior to sequencing on an Illumina NovaSeq 6000, libraries go through a bead-based purification step, and the quality is assessed using the Agilent 2100 Bioanalyzer (Agilent Technologies, Palo Alto, CA). The raw output data are quality controlled, normalized, and converted into Normalized Protein eXpression (NPX), Olink's proprietary unit of relative abundance. Data normalization is performed using an internal extension control and an external plate control to adjust for intra- and inter-run variation. All assay validation data (detection limits, intra- and inter-assay precision data, predefined values, etc.) are available on the manufacturer's website (www.olink.com).

Insulin assay

Insulin from CSF was measured by ELISA using Mercodia ultrasensitive insulin ELISA kit in triplicate (Catalog No. 10-1132-01). Briefly, 25 μL of samples and calibrators (0.15–20 mU/L) were mixed with 100 μL of enzyme conjugate in a precoated 96-well plate and incubated on a plate shaker (800 rpm) for 1 h at room temperature. The plate was then washed and added by substrate and stop solution. The optical density was read at 450 nm with a plate reader.

QUANTIFICATION AND STATISTICAL ANALYSIS

Pharmacokinetic methods

Pharmacokinetic parameters for ketamine, NK, and (2*S*,6*S*;2*R*,6*R*)-HNK were calculated by direct observation and by noncompartmental analysis using Phoenix WinNonlin (version 8, Certara USA, Inc.). The AUC was determined using the "linear up, log down". The outcome of interest was the ratio between CSF and plasma AUC. Timepoints through 1680 min were used. The following pharmacokinetic parameters were obtained: elimination rate constant (λZ), determined by calculating the absolute value of the slope of the log-linear regression plasma concentration-time plot using a minimum of three concentrations along the elimination phase; plasma elimination half-life ($T_{1/2}$), calculated as 0.693/λZ; the maximum observed concentration (C_{max}); the corresponding peak time (T_{max}); AUC from time zero to 1,440 min (AUC0-1440 min); AUC_{last}, calculated using the last observed pharmacokinetic timepoint; AUC, extrapolated to infinite time; distribution volume, calculated as dose/(AUC_{last}* λZ); and clearance, calculated as dose/AUC.

Data analysis

This was an exploratory analysis in a small sample with many comparisons and is therefore intended to be hypothesis generating. Consistent with the current suggestion of the American Statistical Association,[117] we eschew "statistical significance" in favor of exact uncorrected p values alongside the magnitude of the parameter estimate and its precision (the 95% CI). We provide full listings of exact p values so that readers may choose to apply their correction method of choice if they deem it necessary. Given the large number of comparisons, we employed an *ad hoc* thresholding method for reporting in-text, which was to select features for which at least two consecutive timepoints had parameter estimates that differed from zero with a p value $\leq$0.01. However, all comparisons are reported in the supplementary tables (Table S6). AUC was calculated via trapezoidal rule using the R package PK.[118] A linear mixed model with a random subject-level intercept and a fixed effect of time were used to model all available data, which were natural-log transformed. The parameters of interest were the slopes indicating difference from baseline for each timepoint. The CSV file has all of the estimates for change from baseline, but the PDF has figures for only the features where at least two consecutive changes had $p < 0.01$. Linear mixed models were implemented with R package lme4.[119]

Statistical analysis of proteomic data

A univariate analysis by time was carried out. This is the mixed model estimating the average change from baseline at each timepoint. The CSV file has all of the estimates for change from baseline, but the PDF has figures for only the features where at least two consecutive changes had $p < 0.05$. A pareto scaled variable was analyzed.

ADDITIONAL RESOURCES

This clinical trial (NCT03065335) is registered with www.clinicaltrials.gov (https://clinicaltrials.gov/study/NCT03065335?term=NCT03065335&rank=1).